Canadian Science Publishing

ARTICLE

Functional analysis of co-expression networks of zebrafish *ace2* reveals enrichment of pathways associated with development and disease

Ayse Gokce Keskus, Melike Tombaz, Burcin Irem Arici, Fatma Betul Dincaslan, Afshan Nabi, Huma Shehwana, and Ozlen Konu

Abstract: Human Angiotensin I Converting Enzyme 2 (ACE2) plays an essential role in blood pressure regulation and SARS-CoV-2 entry. ACE2 has a highly conserved, one-to-one ortholog (*ace2*) in zebrafish, which is an important model for human diseases. However, the zebrafish *ace2* expression profile has not yet been studied during early development, between genders, across different genotypes, or in disease. Moreover, a network-based meta-analysis for the extraction of functionally enriched pathways associated with differential *ace2* expression is lacking in the literature. Herein, we first identified significant development-, tissue-, genotype-, and gender-specific modulations in *ace2* expression via meta-analysis of zebrafish Affymetrix transcriptomics datasets ($n_{datasets}$ = 107); and the correlation analysis of *ace2* meta-differential expression profile revealed distinct positively and negatively correlated local functionally enriched gene networks. Moreover, we demonstrated that *ace2* expression was significantly modulated under different physiological and pathological conditions related to development, tissue, gender, diet, infection, and inflammation using additional RNA-seq datasets. Our findings implicate a novel translational role for zebrafish *ace2* in organ differentiation and pathologies observed in the intestines and liver.

Key words: zebrafish, *ace2*, transcriptome, network analysis, meta-analysis.

Résumé : L'enzyme humaine de conversion de l'angiotensine 2 (ACE2) joue des rôles essentiels dans la régulation de la tension artérielle et l'entrée du SARS-CoV-2. L'ACE2 possède un orthologue direct très conservé (*ace2*) chez le poisson-zèbre, un organisme modèle important dans l'étude des maladies humaines. Cependant, le profil d'expression du gène *ace2* chez le poisson-zèbre n'a pas encore été étudié au cours des premiers stades de développement, chez les deux sexes, au sein de différents génotypes et en cas de maladie. De plus, aucune méta-analyse fondée sur les réseaux n'a encore été faite pour identifier les sentiers fonctionnels qui sont enrichis en fonction de l'expression différentielle du gène *ace2*. Dans ce travail, les auteurs ont d'abord identifié des modulations spécifiques dans l'expression d'*ace2* en fonction du stade de développement, du tissu, du génotype ou du sexe via une méta-analyse des jeux de données transcriptomiques Affymetrix pour le poisson-zèbre (n_{jeux} = 107). Une analyse de corrélation des profils d'expression méta-différentiels d'*ace2* mis a au jour des réseaux géniques locaux distincts, à corrélation à la fois positive et négative, qui reflétaient un enrichissement fonctionnel. De plus, les auteurs ont démontré que l'expression d'*ace2* était modulée de manière significative en fonction des conditions physiologiques et pathologiques liées au stade de développement, au tissu, au sexe, à la diète, à l'infection et à l'inflammation en utilisant des jeux de données RNA-seq additionnels. Ces résultats impliquent un rôle traductionnel inédit pour le gène *ace2* du poisson-zèbre dans la différentiation des organes et des pathologies observées dans l'intestin et le foie. [Traduit par la Rédaction]

Mots-clés : poisson-zèbre, *ace2*, transcriptome, analyse de réseaux, méta-analyse.

Received 26 March 2021. Accepted 22 September 2021.

A.G. Keskus. Interdisciplinary Program in Neuroscience, Bilkent University, Ankara, Turkey.
M. Tombaz, B.I. Arici, and F.B. Dincaslan. Department of Molecular Biology and Genetics, Bilkent University, Ankara, Turkey.
A. Nabi. Department of Molecular Biology and Genetics, Bilkent University, Ankara, Turkey; Faculty of Engineering and Natural Sciences, Sabancı University, Istanbul, Turkey.
H. Shehwana. Department of Molecular Biology and Genetics, Bilkent University, Ankara, Turkey; Department of Biological Sciences, National University of Medical Sciences, Rawalpindi, Pakistan.
O. Konu. Interdisciplinary Program in Neuroscience, Bilkent University, Ankara, Turkey; Department of Molecular Biology and Genetics, Bilkent University, Ankara, Turkey; UNAM-Institute of Materials Science and Nanotechnology, Bilkent University, Ankara, Turkey.
Corresponding author: Ozlen Konu (email: konu@fen.bilkent.edu.tr).

Introduction

ACE2 and ACE, involved in angiotensin conversion, are integral elements of renin-angiotensin signaling (RAS) in multiple tissues. Recent studies have shown that RAS is not only present in the kidney or adrenal glands but also functional in other tissues with significant roles in multiple pathologies, including cancer (Cheng and Liu 2019; Nehme et al. 2019; Pinter and Jain 2017; Rasha et al. 2019). The role of ACE2 and ACE in the regulation of hypertension is well known (Hamming et al. 2007), and ACE2 has recently become the focus of intense research due to its function as a receptor of SARS-CoV-2 entry in COVID-19 (Ziegler et al. 2020). In addition, *ACE2* expression is tissue-specific; for example, recent findings from single-cell RNA-seq studies show that *ACE2* is highly expressed in type II pneumocytes and intestinal enterocytes, in which SARS-CoV-2 can replicate (Ziegler et al. 2020).

In addition to mammalian models, zebrafish have recently been used to study *ace2* expression and function. Zebrafish *ace2* is highly conserved in sequence and structure to its mammalian counterparts and exists as the only copy in zebrafish with a duplicated genome (Chou et al. 2006). Furthermore, a recent study, phylogenetically comparing genes co-expressed with *ace2* based on zebrafish single-cell RNA-seq tissue data revealed that RAS signaling is also conserved between humans and zebrafish (Postlethwait et al. 2021). However, to our knowledge, no study has investigated the changes in *ace2* expression over zebrafish embryonic and larval developmental stages, between genders, and in different whole adult tissues as well as across different genotypes, treatments, or pathologies. Accordingly, a meta-analysis of differential expression of zebrafish *ace2*, performed across public datasets, may reveal important functionally enriched networks (Shehwana and Konu 2019).

Co-expression analysis is a widely used and effective method based on the guilt-by-association principle to identify the regulatory mechanisms of transcription under certain conditions. Several methods have been proposed to perform co-expression analysis, such as effect size, rank, or p-value combinations, and random sampling (Evangelou and Ioannidis 2013; Gur-Dedeoglu et al. 2008; Kolde et al. 2012; Tseng et al. 2012). Because traditional co-expression analysis methods are based on using the expression values from individual samples, preprocessing steps may be required to remove batch effects between datasets. However, data merging with an increasing number of datasets may not be optimal (Cheung and Vijayakumar 2016), and when combining a heterogeneous set of datasets it requires different approaches (Ter Veer et al. 2019). Recent network-based methods have proposed combining the individual co-expression network of each dataset, calculated separately; however, these methods are computationally expensive for a large collection of datasets (Ter Veer et al. 2019). A simpler and widely used methodology is to use or compare the logFC values (as the mean expression value normalized to internal control) obtained for each dataset that may come from numerous conditions, which has been used in different contexts, including miRNA target prediction, toxicogenomic patterns, and compound similarity matrices (Kramer et al. 2020; Yoon et al. 2019; Zhou et al. 2018; Cheng and Yang 2013). Here, we combined these two methods, that is, logFC comparison and co-expression network, and performed a pairwise correlation analysis between *ace2* and other genes using logFC values obtained from re-analysis (limma) of public zebrafish Affymetrix datasets (GEO), followed by network enrichment.

Briefly, we hypothesized that significantly enriched functional local networks extracted based on the differential expression profile of *ace2* across divergent contexts can provide a better understanding of zebrafish *ace2* function. Using the wealth of transcriptomic data present in the zebrafish literature, we aimed to identify the development-, tissue-, gender-, and genotype-specific differences in *ace2* expression and extract its co-differentially expressed transcriptome in zebrafish using available datasets. We also investigated whether *ace2* was tissue-specific and found that it was expressed the most in the intestines followed by the liver, although highly variable. We then performed comparisons between relevant datasets using local network signatures (STRING) of genes co-expressed with *ace2*, which helped prioritize the positively and negatively ranked local functional pathways with which *ace2* was associated with development, intestinal differentiation, and variable liver expression. Using additional datasets, we showed that zebrafish *ace2* was also modulated in different liver and intestinal pathologies, demonstrating its translational importance.

Methods

Co-differential expression analysis using Affymetrix Zebrafish Chip datasets (GPL1319)

Raw CEL files for all available datasets for GPL1319 were obtained from the NCBI GEO database (Fig. S1[1]) (Barrett et al. 2013). Groups containing at least two samples were used for comparisons, and datasets with no comparable groups were excluded ($n_{datasets}$ = 107). Normalization of CEL files for each study was performed separately using rma in the *affy* package (Gautier et al. 2004). From the 107 datasets, 344 two-group comparisons were manually generated using the following rules: (*i*) each experimental group was compared to the corresponding control group; (*ii*) experimental groups with double mutation or morpholino treatment were compared to each of the single mutation/morphant

[1]Supplementary data are available with the article at https://doi.org/10.1139/gen-2021-0033.

groups; (*iii*) only control (or wild type) groups from different tissues, developmental time points, or gender were compared with each other; (*iv*) for the time series, all other groups were compared to the group with the earliest time point only. Differential expression analysis using limma was conducted for each of the manually generated two-group comparisons with the normalized datasets (Ritchie et al. 2015). A matrix of logFC values, X_{logFC}, was obtained, where each row corresponded to a gene and each column corresponded to one of the limma comparisons. The average logFC values for each gene were calculated across 344 comparisons, and the distribution was plotted as a histogram. A Pearson correlation coefficient ($r_{ace2\text{-}logFC}$) was then calculated between *ace2* and every other gene found in X_{logFC}. Furthermore, $r_{ace2\text{-}logFC}$ values were used to identify STRING-enriched local networks, that is, small protein–protein interaction networks with 5 to 200 members, obtained through hierarchical clustering of the human protein–protein network and named according to the consensus annotations of proteins found in subnetworks (Szklarczyk et al. 2019). In addition, limma comparisons in which *ace2* was differentially expressed were identified upon setting the FDR and logFC thresholds stringently (adj. p-value < 0.05, abs(logFC) > 0.5).

Identification of tissue-specific expression patterns of ace2 in zebrafish adult tissues

Raw data for selected tissue datasets (Table S1[1]) were obtained from SRA (Chen et al. 2020*a*) and analyzed using Seven Bridges Cancer Genomics Cloud (CGC; https://www.cancergenomicscloud.org/). The reads were aligned using the Star Alignment tool (Dobin et al. 2013). The HTSeq tool (Anders et al. 2015) was used to retrieve count data. Raw count data were normalized using the RPKM function from the *edgeR* package in R (McCarthy et al. 2012). Samples from the same tissue and from different datasets were visualized by plotting the scores from the first two dimensions of principal component analysis (PCA) and hierarchical clustering. Tau was used as the tissue-specificity index, as described previously (Kryuchkova-Mostacci and Robinson-Rechavi 2017).

Dataset collection for investigating sexual dimorphism, and intestinal and liver development and disease

Zebrafish transcriptomics datasets selected from NCBI GEO or Expression Atlas (Papatheodorou et al. 2020) according to their relevance to sexual dimorphism, liver and gut development, and disease/treatments are summarized in Table S2[1]. Series matrix files for four datasets of GPL14664 (GSE113241 (Alvarez-Rodriguez et al. 2018), GSE112272 (Jia et al. 2019), GSE73233 (Forn-Cuni et al. 2017), and GSE100583 (Holden and Brown 2018)) and RPKM normalized data of GSE74244 (Aramillo Irizar et al. 2018), GSE118076 (San et al. 2018), and GSE24616 (Domazet-Loso and Tautz 2010) were obtained from GEO and used for statistical analysis after logarithmic (log2) transformation. The expression of *ace2* in the E-ERAD-475 dataset was obtained from Expression Atlas (White et al. 2017). ANOVA followed by multiple test correction (Tukey's HSD) was used for statistical analyses, as indicated in the figure legends. Raw count data of GSE82200 (Koch et al. 2018), GSE83195 (Schall et al. 2017), and GSE123439 (Chen et al. 2020*b*) were obtained from NCBI GEO, *Deseq2* package was used for differential gene expression analysis, and regularized log (Rlog) normalized expression values were used for visualization (Love et al. 2014).

Condition-specific co-expression analysis

To generate a co-expression network of *ace2*, a Pearson's correlation coefficient, called r_{ace2}, was calculated between *ace2* and each gene based on the log2 transformed expression values, generating a vector of r_{ace2} values for each comparison studied, namely, (*i*) larval development, using GSE24616 (2–8 dpf) and GSE38575 (EtOH-treated samples only; 2–7 dpf) datasets; (*ii*) intestinal expression, using GSE35889 and GSE12189 (GFP+ samples only); and (*iii*) expression in liver, using GSE74244 (liver samples only) and GSE100583, separately (Fig. S2, Table S2[1]). The r_{ace2} value with the minimum p-value was selected for multiple probe sets with the same Ensembl ID.

Comparative network enrichment analysis (CNEA)

Ensembl IDs and each of the condition-specific r_{ace2} values were used to identify local network clusters using STRING enrichment analysis (Szklarczyk et al. 2015). After obtaining enrichment results for each dataset, a comparative network enrichment analysis (CNEA) of STRING local networks was performed to identify consistently enriched local networks common in both datasets and visualized via scatter plots (FDR < 0.01). Enriched local networks with the largest gene set were selected in the presence of multiple local networks with the same name. A local network interaction graph was then generated using networks significantly (FDR < 0.01) enriched in both datasets, where nodes represent local networks and edges, the number of shared genes between local networks. The generated graph was then clustered in Cytoscape using the Markov cluster algorithm (MCL) (Shannon et al. 2003). Selected local networks were visualized in detail, where each node on the specific STRING local network data referred to a gene and was colored according to its r_{ace2}, that is, the correlation with *ace2* expression. In addition, a GO term enrichment analysis was performed for liver datasets using the *clusterProfiler* package in R (Yu et al. 2012).

Results

Re-analysis of zebrafish GPL1319 datasets revealed conditions in which *ace2* expression was significantly modulated

Upon re-analysis of publicly available datasets from the GPL1319 platform ($n = 107$ with 344 pairwise group

Table 1. GPL1319 datasets in which zebrafish *ace2* with a probe set ID "Dr.20290.1.A1_at" was significantly differentially expressed (FDR (adj. p-value) < 0.05 and abs(logFC) > 0.5).

Dataset ID	logFC	p-value	adj. p-value	Comparison
GSE14979	−3.92	8.7E-06	2.1E-04	Ovary vs. Female Body
GSE14979	−3.88	1.0E-06	1.5E-05	Testis vs. Male Body
GSE13158	−3.77	5.7E-16	2.1E-13	50 μM *ERbeta2* vs. Control morpholino
GSE17711	−1.86	4.8E-06	1.1E-03	*cdipt* Mutant vs. Wild type
GSE55339	−1.43	8.5E-05	1.2E-02	*uhrf1* Mutant vs. Wild type
GSE12214	−1.10	3.0E-04	4.3E-03	1000 μg MCLR vs. Control ethanol
GSE11493	−1.06	1.6E-03	1.1E-02	MPNST (p53mut) vs. Seminoma
GSE14979	−0.90	1.1E-02	2.0E-02	Ovary vs. Testis
GSE4859	−0.81	8.3E-05	5.1E-03	Whole ovary 100 ppb TCDD vs. Whole ovary control
GSE12214	−0.80	4.1E-03	4.2E-02	100 μg MCLR vs. Control ethanol
GSE32360	−0.64	2.2E-02	3.6E-02	24 hpf mock LNA vs. 1 hpf mock LNA
GSE18830	−0.63	2.1E-03	6.0E-03	75% Epiboly vs. 30% Epiboly
GSE18830	−0.56	1.0E-03	2.4E-03	Tail Bud vs. 30% Epiboly
GSE12189	2.92	7.9E-03	4.8E-02	6 dpf (GIT) vs. 2 dpf (GIT)
GSE12189	3.05	9.6E-06	5.4E-04	6 dpf (not-GIT) vs. 2 dpf (not-GIT)
GSE12189	3.85	4.5E-06	3.2E-04	3 dpf (GIT) vs. 3 dpf (not-GIT)
GSE12189	3.95	9.0E-06	5.6E-03	3 dpf (GIT) vs. 2 dpf (GIT)
GSE12189	4.68	5.3E-04	1.2E-02	4 dpf (GIT) vs. 2 dpf (GIT)
GSE35889	7.58	5.7E-07	3.6E-04	*cdx1b* Transgenic vs. Wild type

Note: MCLR, MPNST, TCDD, LNA, and GIT refer to microcystin-LR, malignant peripheral nerve sheath tumor, 2,3,7,8-Tetrachlorodibenzo-p-dioxin, locked nucleic acid, and gastrointestinal tract, respectively.

Fig. 1. (A) Carboxypeptidase and (B) intraflagellar networks colored according to $r_{ace2\text{-}logFC}$ values across GPL1319 datasets ($n_{datasets}$ = 107; $n_{comparison}$ = 344).

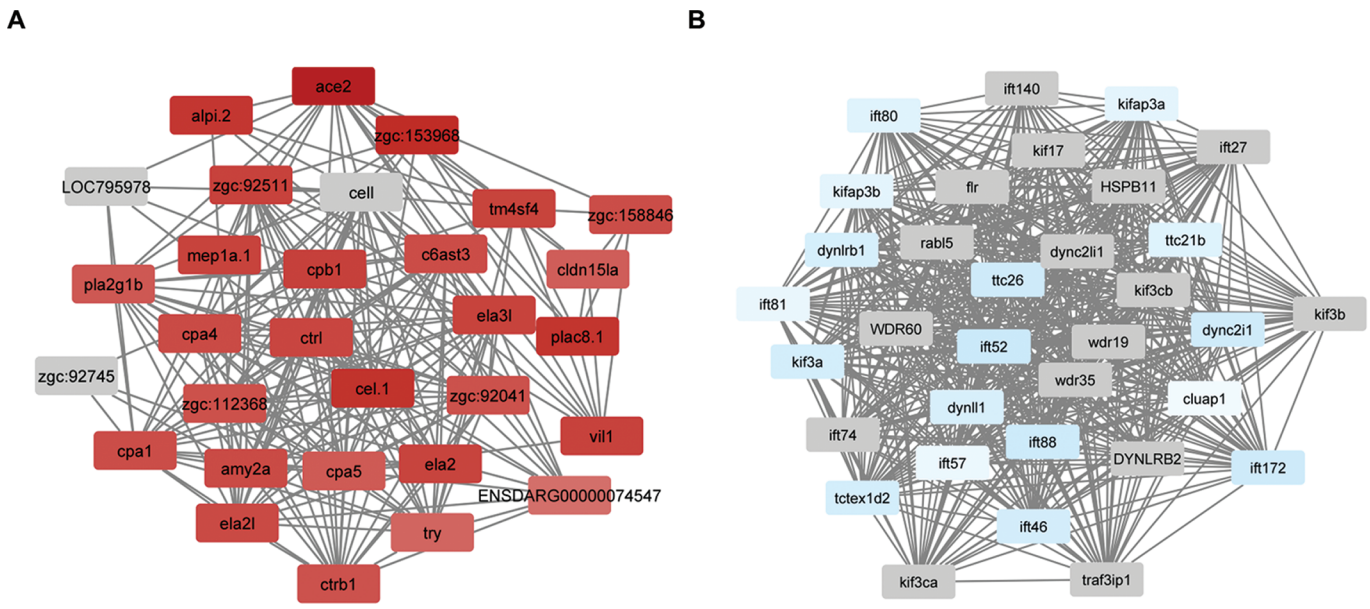

comparisons), *ace2* expression was found to be differentially expressed in 19 pairwise group comparisons from 11 different datasets relevant to sexual dimorphism, estrogen signaling, embryogenesis, and liver and gut development (Table 1) (Froehlicher et al. 2009; Heiden et al. 2008; Hu et al. 2013; Jacob et al. 2015; MacInnes et al. 2008; Rogers et al. 2011; Small et al. 2009; Soni et al. 2013; Stuckenholz et al. 2009; Thakur et al. 2014; Okuda et al. 2010). The logFC matrix for all zebrafish genes across 344 comparisons was generated, and row (i.e., gene) mean and coefficient of variation (CV) values were found to be distributed symmetrically around 0 (Figs. S3A–S3B[1]). The co-differential expression vector of *ace2*, $r_{ace2\text{-}logFC}$, was used to obtain STRING local network clusters, which revealed that genes positively correlated with *ace2* were enriched in carboxypeptidase activity (Fig. 1A), intestinal hexose absorption, villin and keratin, and fibrin clot formation associated sub-groups (Fig. S4A[1]),

Fig. 2. *ace2* expression patterns during developmental stages from (A) GSE24616, where min, d, and h refer to minutes, days, and hours, respectively, and (B) GSE38575, where EtOH, VD, and dpf refer to ethanol, vitamin D, and days post-fertilization, respectively. (C) Correlation between significantly modulated STRING local network enrichment scores obtained using r_{ace2} values using developmental datasets.

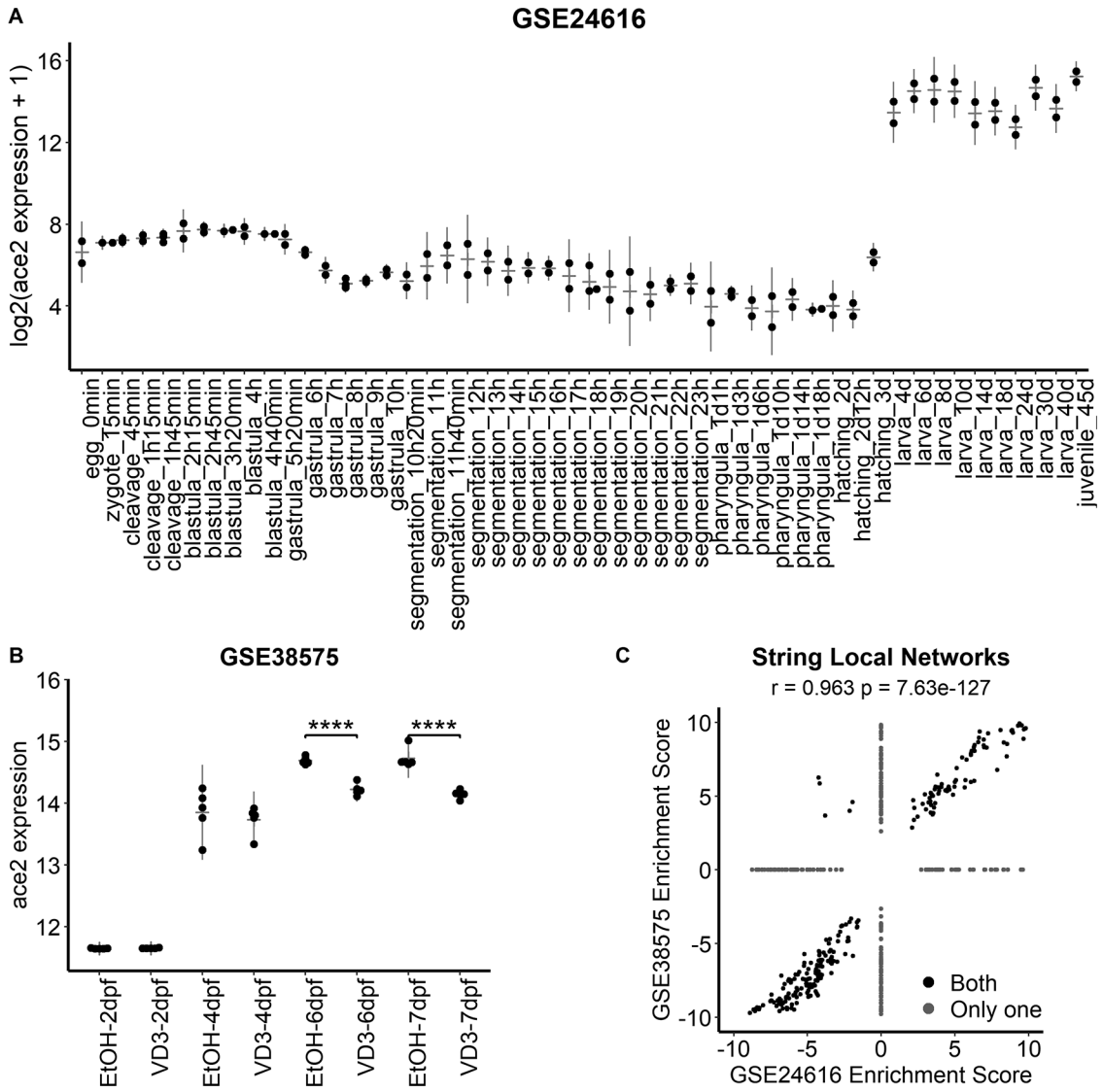

whereas those negatively correlated belonged to cilium assembly (Fig. 1B), microtubule organization pathways, and chromatin-modifying enzymes (Fig. S1A[1]). Ten genes were represented in the GPL1319 platform out of 28 RAS pathway genes (Postlethwait et al. 2021), and eight of them were found to be positively correlated with *ace2*, with a correlation coefficient ranging from 0.46 to 0.85.

ace2 expression in zebrafish is developmentally modulated

Analysis of GPL1319 datasets revealed that *ace2* expression decreased throughout gastrulation (GSE18830, GSE32360; Table 1), which was supported by re-analysis of GSE24616 (Fig. 2A) and E-ERAD-475 (Fig. S1B[1]). In addition, we found that *ace2* was expressed at low levels during embryogenesis and started to increase at 3 dpf and thereafter until 4 dpf, after which it was steadily expressed at high levels (Fig. 2A, Fig. S4B[1]). Analysis of yet another dataset (GSE38575) supported this finding of a significant increase in *ace2* expression after 3 dpf in zebrafish (Fig. 2B). The STRING local network enrichment scores based on r_{ace2} values (between expression profile of *ace2* and that of every other gene), obtained separately for GSE24616 (2–8 dpf) and GSE38575 (untreated; 2–7 dpf) zebrafish embryonic development datasets, were significantly correlated with each other (r = 0.963, p-value = 7.63e-127; Figs. 2A–2C). Network clustering helped us define pathways modulated at the time of *ace2* induction during the development of early zebrafish larvae. Accordingly, networks enriched with genes positively correlated with *ace2* included pathways related to intestinal hexose absorption, vitamin D metabolism, carboxypeptidases, interleukin signaling, phenylalanine/tyrosine

Fig. 3. Top 15 positively and negatively enriched networks using r_{ace2} values obtained using STRING local network analysis of GSE24616 and GSE38575 focusing on zebrafish early development.

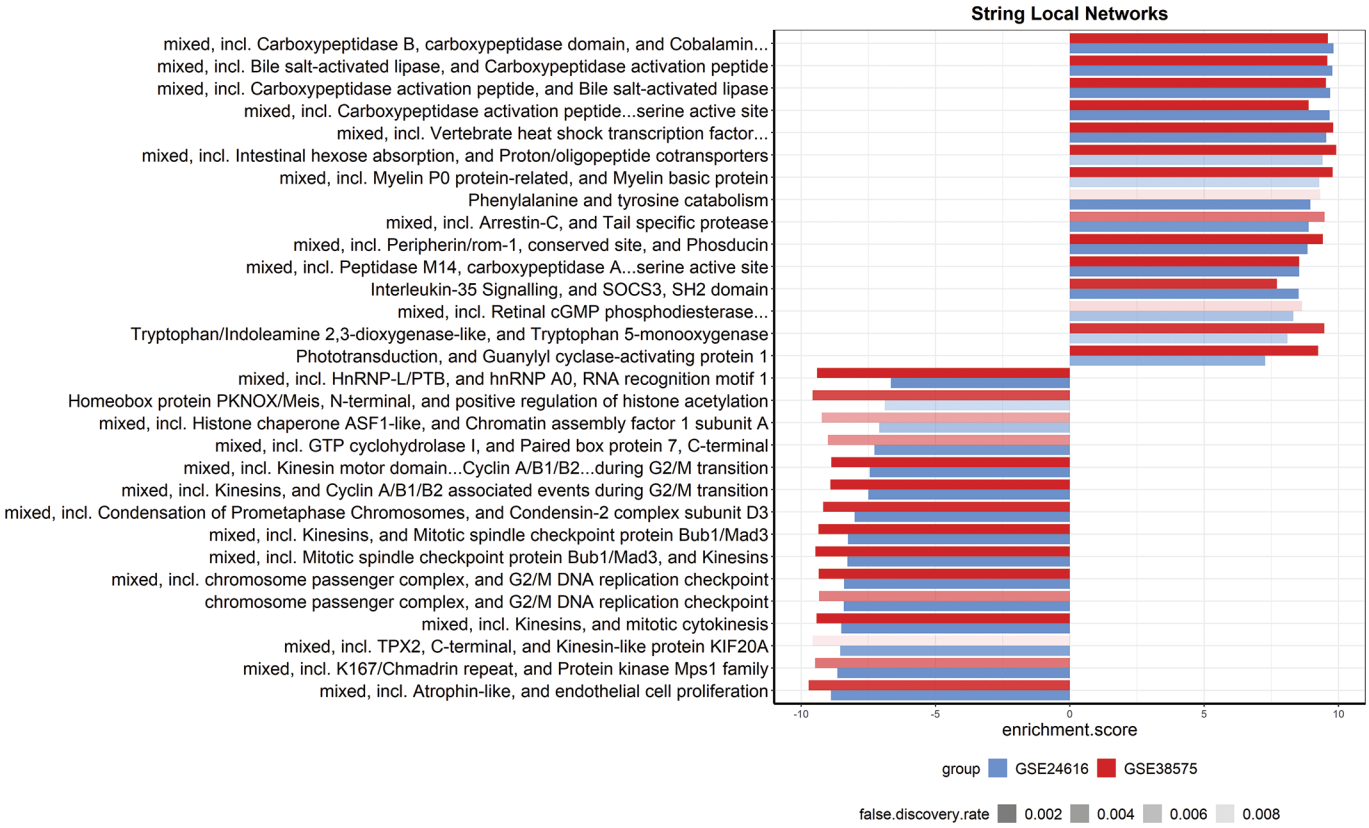

catabolism, peptide ligand binding, dopamine receptors, phototransduction, and common fibrin clot/fibrinolysis (Fig. 3, Fig. S5[1]). On the other hand, networks enriched with negatively correlated genes included terms such as chromosome segregation, cilium assembly, DNA double-strand break and replication, homeobox, alternative splicing, and endothelial cell proliferation (Fig. 3, Fig. S6, Table S3[1]). We then generated graphs with positively and negatively enriched networks separately, in which the edge weights represent the number of genes common in both networks to obtain a more comprehensive view of the ace2's functions. Here, we found that interleukin-20, interleukin-6, interleukin-21, and interleukin-35 signaling networks formed a network, and some of the genes involved in vitamin D metabolism along with SLC-mediated transmembrane transport networks were also enriched (Fig. 4). Networks relevant to chromatin segregation clustered together with the checkpoint-associated networks, while cilium assembly and microtubule organization formed separate networks, as in the case of DNA damage response-associated networks (Fig. 5).

ace2 expression in zebrafish is sexually dimorphic and tissue-specific

One of the most prominent findings of the GPL1319 dataset meta-analysis was the identification of sexual dimorphism in zebrafish *ace2* expression, as shown in Table 1 (GSE14979, Table 1). Interestingly, gonads had lower *ace2* expression when compared with the rest of the body regardless of sex, while testis had relatively higher *ace2* levels than the ovary (GSE14979, Fig. S7A[1]). Moreover, *ace2* expression decreased in the presence of a morpholino for *ERBeta2* (*esr2a*) (GSE13158, Table 1), which was previously shown to be essential for female sexual maturation and early follicle generation (Lu et al. 2017; Wu et al. 2020). We then re-analyzed the GSE24616 dataset for *ace2* expression in adult zebrafish over time and found that *ace2* was highly expressed in juveniles and early adulthood (90 dpf) (Fig. 6A). Moreover, males exhibited high *ace2* expression regardless of age, while females showed a steady decrease with aging until 9 months (Fig. 6A; adj. p-value <0.0001 (age), adj. p-value < 0.0001 (gender), adj. p-value = 0.43 (interaction)). However, after 9 months, *ace2* levels were indistinguishable between males and females. The results obtained from another dataset, GSE123439, were consistent with the observed significance of sexual dimorphism in gonads (Fig. S7B[1]). In addition, we investigated the tissue-specificity of *ace2* using a collated dataset (Methods for details). Samples from the same tissue and (or) anatomically related organs were clustered together using PCA and hierarchical clustering (Fig. S8[1]). We found that the intestines and liver exhibited relatively high *ace2* expression in comparison with the brain, gills, and kidneys

Fig. 4. Selected common positively enriched networks using r_{ace2} values during zebrafish development. Each node represents an enriched network, and edge weights represent the number of shared genes. Nodes are colored according to their enrichment score.

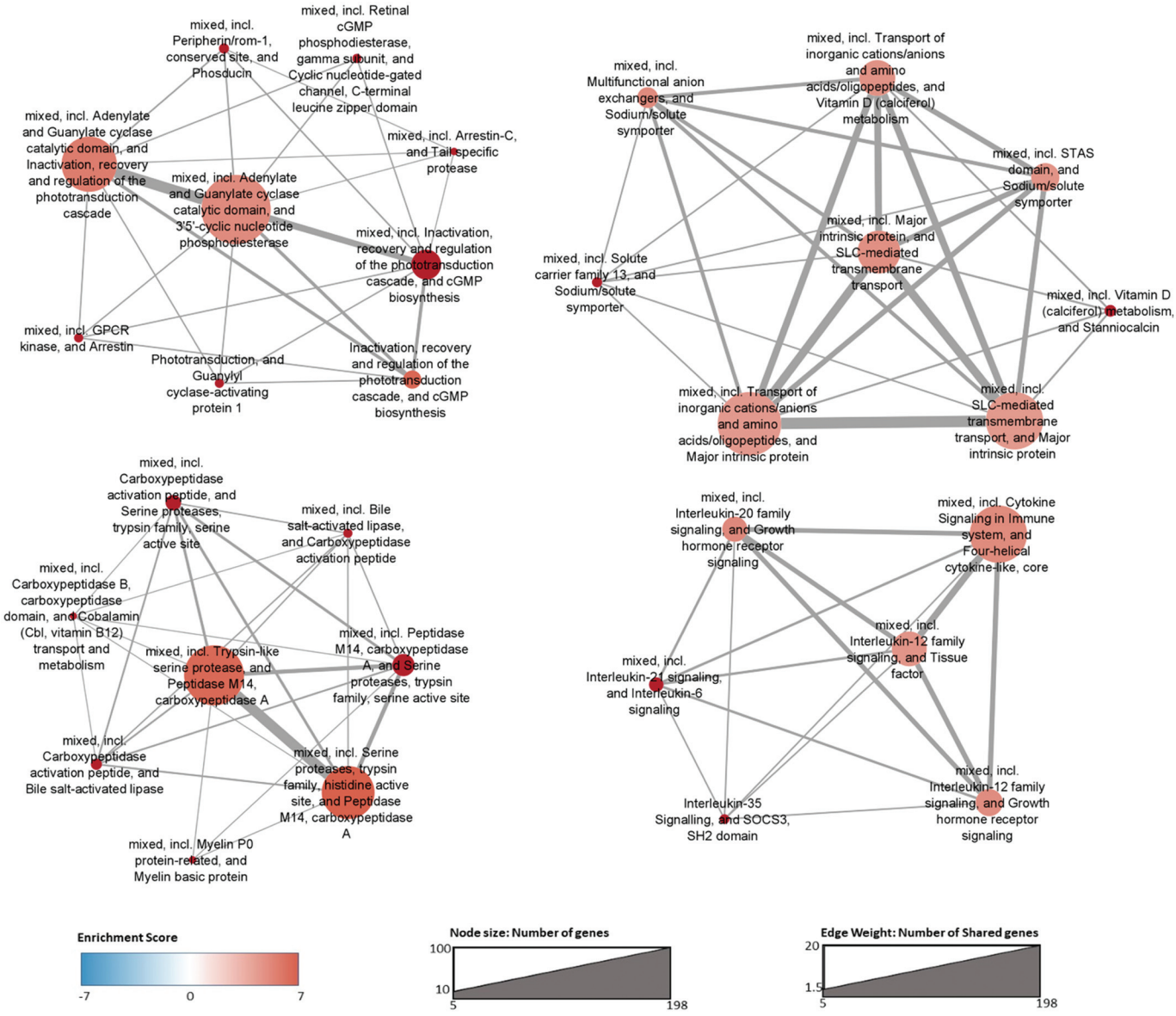

in that descending order (Fig. 6B). Accordingly, zebrafish *ace2* expression was found to have a high tissue-specificity index value (Tau) of 0.99 (Kryuchkova-Mostacci and Robinson-Rechavi 2017).

ace2 exhibits the highest expression in the intestines

In accordance with the above tissue-specificity analysis, our meta-analysis of GPL1319 datasets also implicated *ace2* in intestinal development. Indeed, *ace2* expression increased the most in the intestines of the zebrafish overexpression model of *cdx1b*, an intestinal differentiation-related transcription factor (GSE35889, Table 1). Moreover, *ace2* expression increased in GFP+ gastrointestinal tract (GIT) cells of transgenic (Tg(XlEef1a1:GFP)s854) zebrafish larvae at and after 3 dpf compared to 2 dpf (GSE12189, Table 1; Fig. 7A), whereas in GFP– (non-GIT) cells, *ace2* was significantly upregulated at 6 dpf only. Since *ace2* expression also increased in GFP+ cells when compared to GFP– cells at 3 dpf (GSE12189, Table 1; Fig. 7A), we further performed a comparative network enrichment analysis (Methods for details of CNEA) of STRING local networks between the GSE12189 and GSE35889 datasets. The network enrichment scores of the above-mentioned datasets were highly correlated (r = 0.798, p-value = 6.49e-12; Fig. 7B), strengthening the role of *ace2* during intestinal differentiation. The top common networks included those of intestinal hexose absorption, chylomicron assembly, which is a key mechanism for lipid transport in the

Fig. 5. Selected common negatively enriched networks with r_{ace2} values during zebrafish development. Each node represents an enriched network, and edge weights represent the number of shared genes. Nodes are colored according to their enrichment score.

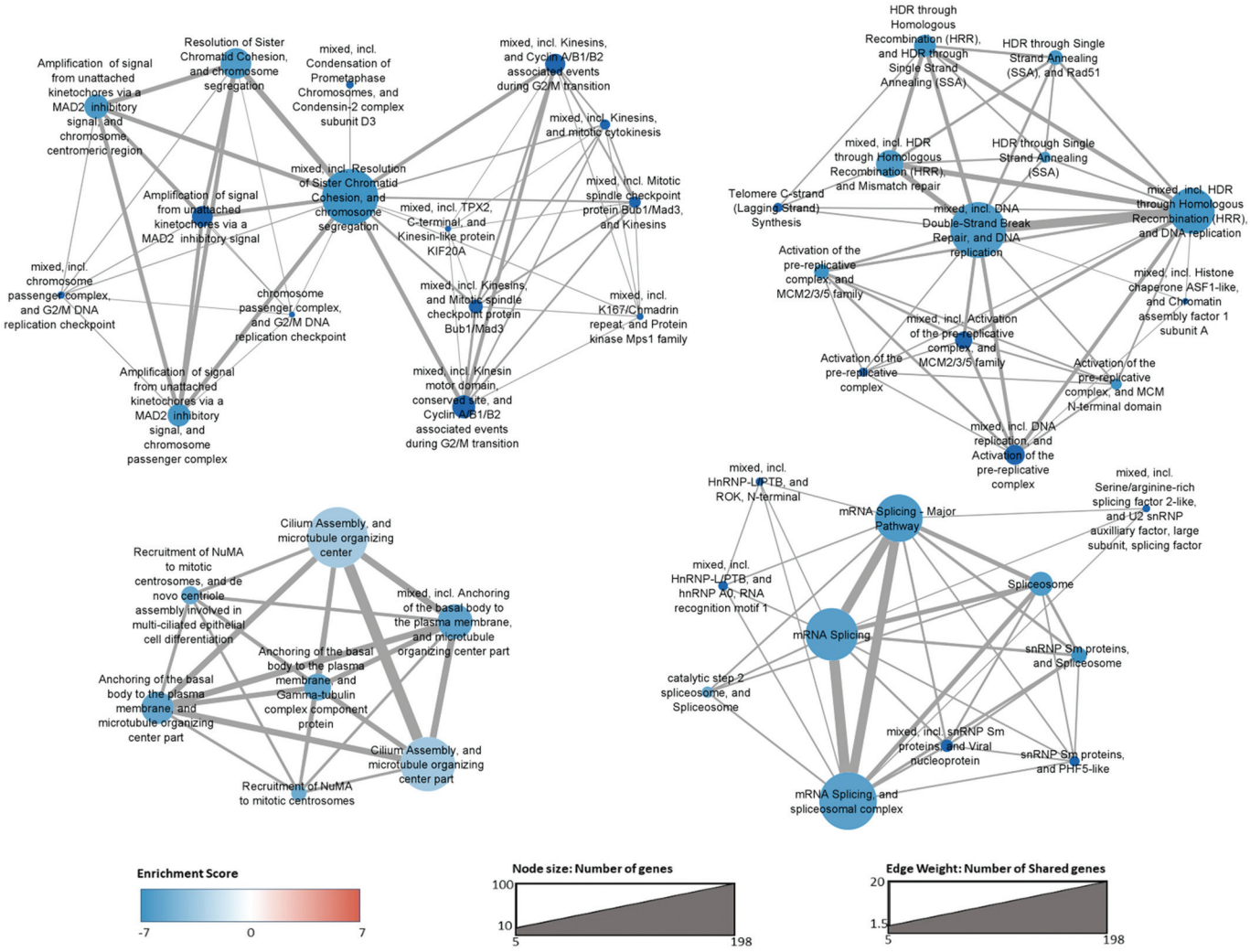

intestines, common pathway of fibrin clot formation and fibrinolysis, fatty acid degradation, and carboxypeptidases (Fig. 7C, Fig. S9[1]). In contrast, negatively correlated genes were enriched in networks of striated muscle contraction and mRNA splicing (Fig. 7C, Fig. S9[1]). Moreover, increases in *ace2* expression were steady over time in late zebrafish larvae with functional intestines (Fig. S10A[1]).

ace2 expression is altered with inflammation

We next focused on available disease model datasets of zebrafish to examine changes in *ace2* expression in inflammation of the intestines and liver. From an intestinal disease perspective, *ace2* was found to be downregulated in the zebrafish model of short bowel syndrome (SBS) (Fig. S10B[1]), which may indicate a possible link between *ace2* expression and inflammatory responses (Johnson et al. 2018; Mutanen et al. 2019; Schall et al. 2017). We further re-analyzed two other expression datasets associated with different inflammatory stimuli in relation to the zebrafish digestive system. No significant alteration in *ace2* expression was observed in response to bacterial colonization (conventionalization (CONVD), *Exiguobacterium* (Exi), or *Chryseobacterium* (Chrys)) in zebrafish embryos (GSE82200, Fig. 8A). However, *ace2* expression significantly increased with immunosuppression in the *myd88* knockout zebrafish embryos showing significant effects for genotype and treatment with a significant interaction between these factors (GSE82200; adj. p-value = 4e-07 (genotype), adj. p-value = 0.03 (germ), adj. p-value = 0.03 (interaction); Fig. 8B). In contrast, *ace2* expression decreased in the kidney with SVCV infection after pre-treatment with β-glucan but not with exposure to lipopolysaccharides (LPS) or polyinosinic:polycytidylic acid (poly (I:C)) exposure (GSE113241, adj. p-value = 0.01 (SVCV), adj. p-value = 0.06 (pre-treatment), adj. p-value = 0.04 (interaction); Fig. 8B). LPS treatment was not effective in the liver, muscle, or kidney, either (Fig. S10C[1]).

Fig. 6. (A) Sexual dimorphic expression pattern in adulthood based on GSE24616 (Simple effect analysis following Two-Way ANOVA results are represented. *, p-value < 0.05). (B) Tissue-specific expression *of ace2* (log2(RPKM + 1)) in the intestines (731.1) and liver (432.8) and the relatively low expression in the gills (1.57), brain (1.08), kidney (0.83), heart (0.62), and muscle (0.49) in the six-month-old zebrafish cohort.

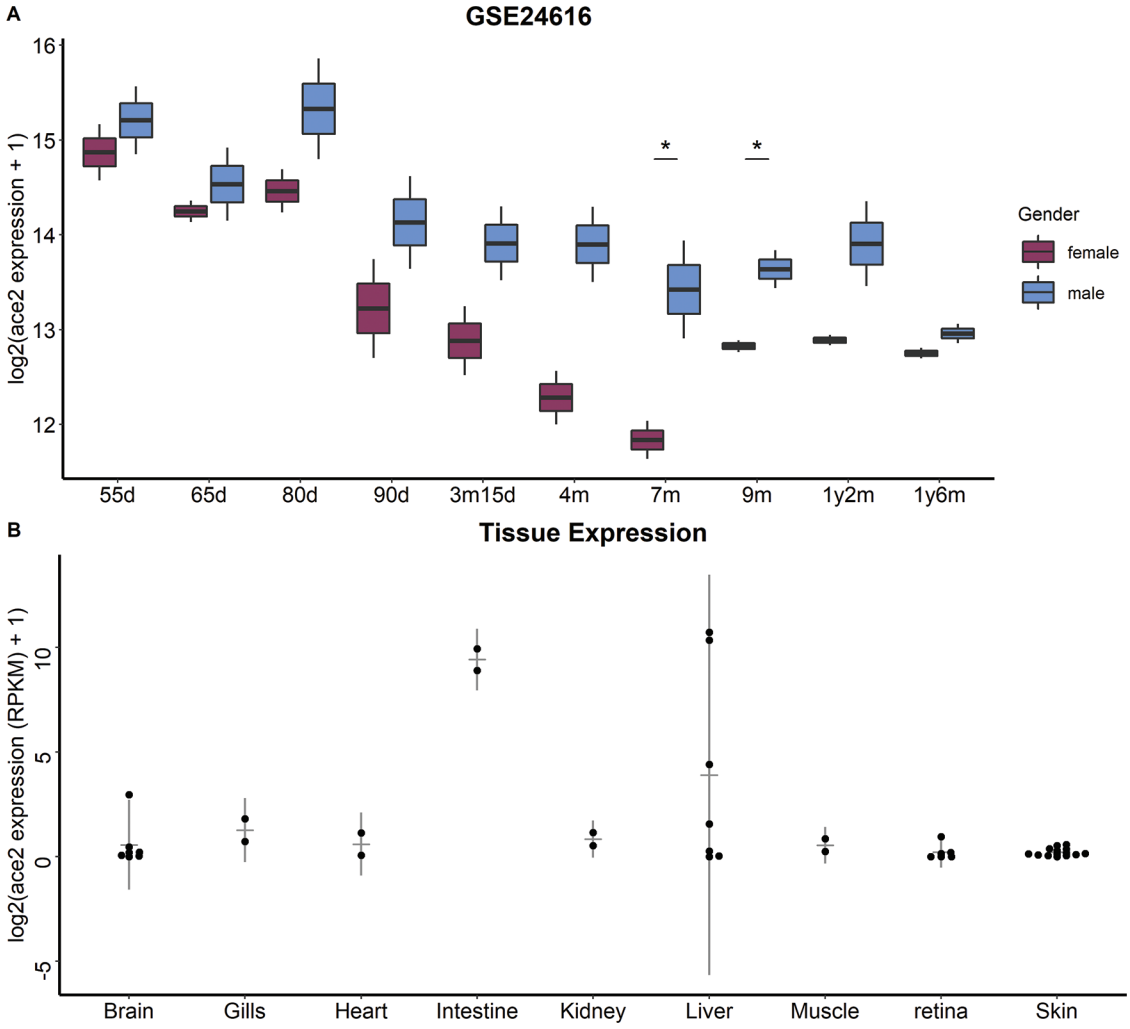

ace2 expression is highly variable in the liver and associated with diet and liver disease

Since *ace2* exhibited the second-highest yet bimodal expression levels in the liver (Fig. 6B; Fig. S11A[1]), we performed GO annotation of genes with high or low r_{ace2} values, obtained by analyzing the GSE74244 dataset (the largest RNA-seq zebrafish cohort for zebrafish adult liver tissue in the GEO database). Significant GO biological processes of genes whose expression levels were positively correlated with that of *ace2* were enriched in metabolism, and in particular, that of the lipid (Fig. S11B[1]), whereas those negatively correlated included the immune response (Fig. S11C[1]). We also showed that liver expression was not sexually dimorphic and could vary regardless of strain and gender using another dataset (GSE100583, Fig. S12A[1]). The results of GO enrichment analysis of GSE100583 were similar in terms of positively correlated genes, yet cilium organization and establishment of cell polarity were found among significantly negatively correlated pathways (Figs. S12B, S12C[1]). CNEA of STRING local networks between these two independent datasets (GSE74244 vs. GSE100583) were highly concordant for a subset of pathways (Fig. 9A, Fig. S13A[1]) and included networks of genes with positive r_{ace2}, such as intestinal brush border proteins (villin and keratin) as well as interferon-stimulated genes (ISG15 antiviral mechanism), carboxypeptidases, and respiratory electron transport and oxidative phosphorylation (Fig. 9A, Fig. S13B[1]). Erythropoietin and the hemoglobin network were among those enriched with negative r_{ace2} values in both datasets (Fig. 9A, Fig. S13B[1]). However, apolipoprotein A/E genes, known to be functional in fat metabolism and immune response, were enriched in both datasets and acted in the opposite direction (Fig. 9A).

We further investigated *ace2* expression in zebrafish under conditions of fasting and refeeding in the liver

Fig. 7. (A) *ace2* expression from GSE12189, where GFP+ and GFP– refer to cells inside and outside of the digestive tract, respectively (limma results are represented. *, adj. p-value < 0.05; **, adj. p-value < 0.01; ***, adj. p-value < 0.001; ****, adj. p-value < 0.0001). (B) Correlation between the significantly modulated STRING local networks obtained using r_{ace2} values in GSE12189 and GSE35889 intestine-specific datasets. (C) Bar plots of significant STRING local network enrichment scores for GSE12189 and GSE35889.

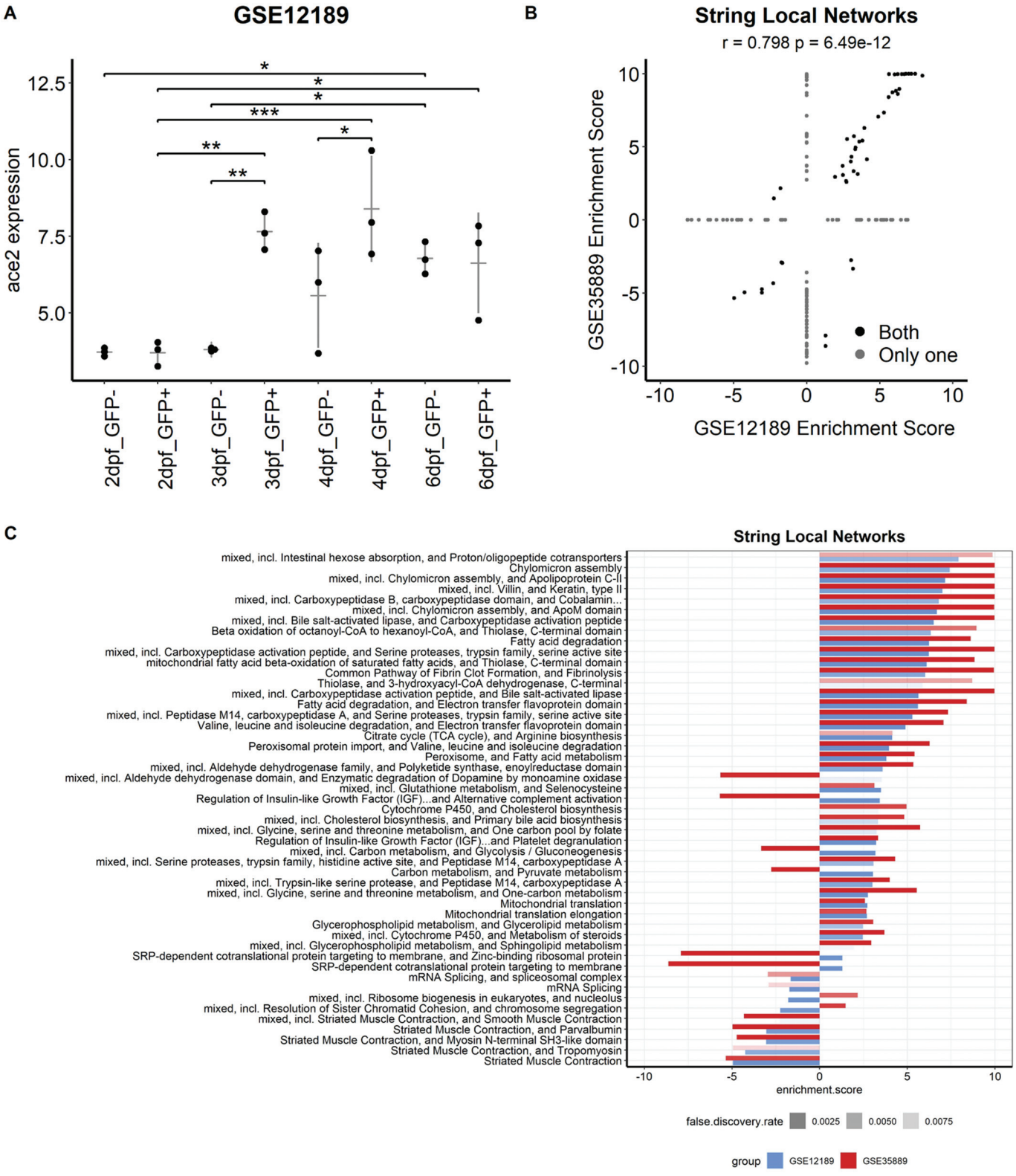

Fig. 8. (A) *ace2* expression during immune response in *myd88* knockout (Myd88KO) model with bacterial colonization (conventionalization (CONVD), *Exiguobacterium* (Exi), and *Chryseobacterium* (Chrys)) (Tukey HSD corrected One-way ANOVA results are represented. *, adj. p-value < 0.05; ****, adj. p-value < 0.0001). (B) *ace2* expression during immune response in viral infection (SVCV: Spring Viraemia Carp Virus) after pre-treatment with the viral medium (MEM), β-glucans, lipopolysaccharide (LPS), or polyinosinic:polycytidylic acid (poly (I:C)) (Simple effect analysis following Two-Way ANOVA results are represented. *; p-value < 0.05).

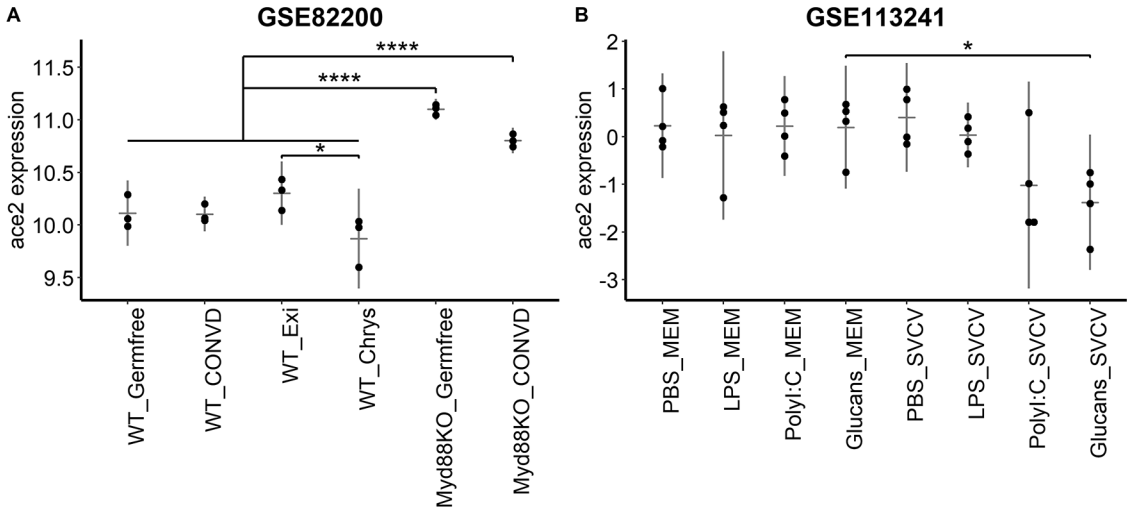

and found *ace2* expression increased when refed after 3 weeks of fasting (Fig. 9B), yet it was not altered when given a high carbohydrate diet (GSE8856 (Robison et al. 2008); logFC = 0.24, adj. p-value = 0.51 (females) and logFC = −0.67, adj. p-value = 0.99 (males)) or under the condition of overfeeding (GSE48806 (unpublished data); logFC = −1.76, adj. p-value = 0.26). To further support the potential involvement of ace2 co-expressed gene network in liver disease, *ace2* expression decreased in the zebrafish non-alcoholic fatty liver disease (NAFLD) model (GSE17711, Table 1) and in response to microcystin-LR, previously shown to cause liver damage (GSE11214, Table 1; Fig. 9C) (Rogers et al. 2011).

Discussion

Zebrafish are widely used as model organisms to understand disease mechanisms because of their high sequence/functional similarity with humans as well as the availability of a wide range of zebrafish genetic models (Gomes and Mostowy 2020; Logan et al. 2018; Mickiewicz et al. 2019; Willis et al. 2016; Shehwana and Konu 2019). Conservation and functional similarity of ace2 and the RAS pathway in zebrafish (Postlethwait et al. 2021) make a disease-focused investigation of zebrafish *ace2* expression essential, yet this has remained unexplored. Our meta-analysis and (or) functional network enrichment approaches with respect to various contexts, including age-, gender-, tissue-specificity, genotype, and disease, make the present study unique and timely.

Our meta-analysis has demonstrated that *ace2* is expressed at low levels during early larval development, yet starts increasing in expression during the differentiation of the liver and intestines (Kimmel et al. 1995). Developmental studies in mice have reported *Ace2* expression at E12.5, with an increasing trend over time in the kidneys, lungs, brain, and heart (Song et al. 2012), while *ACE2* is also expressed in the human intestines, gonads, kidneys, heart, adipose tissue, lung, and liver, in accordance with its multiorgan functionality (Musavi et al. 2020; Wang et al. 2020). In zebrafish, the *ace2* gene is highly expressed in a subcluster of intestinal epithelial cells, where *ace* is also expressed (Postlethwait et al. 2021). In this study, we demonstrated that *ace2* is tissue-specifically expressed in zebrafish adult intestines as *ACE2* in humans (Musavi et al. 2020). Our analyses also suggest a potential role for intestinal differentiation for *ace2*, whose expression is higher in the *cdx1b* transgenic strain exhibiting increased intestinal differentiation (Hu et al. 2013). This finding supports that *cdx1b* could be a transcriptional regulator of *ace2* in zebrafish as *Cdx2*/*CDX2* is in mice (Chen et al. 2020*a*) and humans (Cheng et al. 2008; Flores et al. 2008; Silberg et al. 2000). Moreover, fish larvae with a mutation in the *uhrf1* gene cause non-functional intestines and also exhibit lower levels of *ace2*, further supporting the potential role of *ace2* in intestinal development (Table 1) (Ganz et al. 2019; Marjoram et al. 2015).

Herein, we compared the local enrichment scores between independent datasets (Yildiz et al. 2013) to increase confidence in our context-dependent analysis, that is, *ace2* co-expression in intestinal development and the liver. Such a comparative analysis has proven to be an effective strategy, demonstrating that *ace2* expression is a tightly co-expressed component of carboxypeptidases. Interestingly, this is in accord with the reports proposing the serine protease family of genes, in which

Fig. 9. (A) Bar plots of significant STRING local network enrichment scores for GSE74244 and GSE100583 liver datasets. (B) *ace2* expression in zebrafish livers during fasting and refed conditions. (C) *ace2* expression in zebrafish larvae in response to microcystin-LR (MCLR) exposure (*, p-value < 0.05; **, p-value < 0.01).

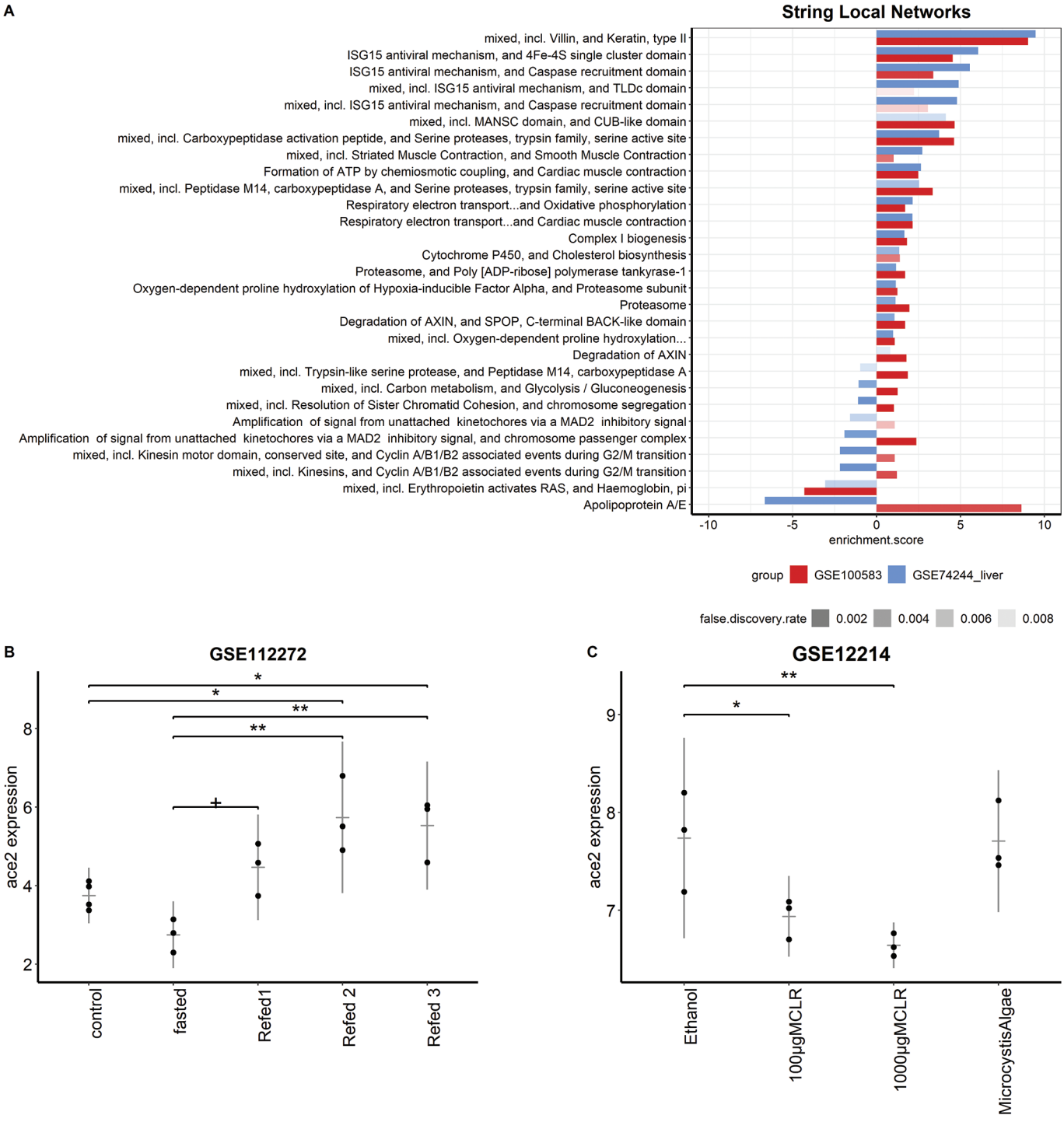

ace2 is part of, as a target for COVID-19 treatment (reviewed in Vargas et al. 2020; Yao et al. 2020). Other networks we identified included fibrinolysis (positive r_{ace2}), and since COVID-19 severity is associated with dysregulation of clot formation (reviewed in Coccheri 2020), we propose that zebrafish larvae can be used to test the effects of SARS-CoV-2 on the fibrinolysis pathway members with which *ace2* is co-expressed during the specific time window of intestinal development.

Interestingly, several studies have previously reported higher *ACE2* expression in cilia of well-differentiated epithelial cells compared to undifferentiated cells in

humans (Jia et al. 2005; Lee et al. 2020*b*; Ziegler et al. 2020). *ACE2* expression is present in motile cilia in human airway epithelial cells (Lee et al. 2020*a*) and is also shown to be affected by SARS-CoV-2 infection (Lee et al. 2020*b*), which causes loss of cilia (Ziegler et al. 2020). Further studies are needed to understand the dynamicity between *ace2* expression and cilium assembly. Indeed, the significant changes observed in *ace2* expression levels at the time of intestinal differentiation also provide an effective translational time frame for testing potential drugs affecting intraflagellar transport and the RAS pathway.

Consistently, our analyses of r_{ace2} in zebrafish have also pointed to the enrichment of respiratory chain-related networks. In support of this, *Ace2* knockout mice have been reported to exhibit disrupted mitochondrial function in pancreatic islets and skeletal muscle cells (Cao et al. 2019; Shi et al. 2018). Transcriptomic analyses of human cornea, retina, and lung datasets suggest that *ACE2* is significantly co-expressed with mitochondrial genes (Yuan et al. 2020). Indeed, Ang II is known to activate NADPH and can stimulate an increase in reactive oxygen species (ROS) in renal cells, while *ACE2*, as a negative regulator of Ang II, has a protective role against ROS (Gava et al. 2009; Gwathmey et al. 2010; Kim et al. 2012). *Ace2* knockout mice also exhibit increased insulin resistance, which can lead to hepatic and oxidative stress (Cao et al. 2014, Gallagher et al. 2008; Gwathmey et al. 2010; Song et al. 2020). The enrichment of ROS-related pathways in our analysis supports the notion that zebrafish can also serve as a model organism to study the potential link between the modulatory role of *ace2* in mitochondrial function and disease.

Our findings have also indicated that the liver is the second-highest *ace2* expressing tissue in zebrafish, yet with a clear bimodal pattern regardless of age (6–42 months) or gender. This bimodality might have arisen from contamination with other tissues, especially the gut and (or) pancreas, and (or) the presence of intrinsic or extrinsic factors in relation to diet, inflammation, or infection. GO enrichment analyses of the positively co-expressed genes of *ace2* revealed the involvement of lipid catabolism as a potential discriminator between low and high *ace2* expressing liver; and in partial support of this, our re-analysis showed that *ace2* levels decrease in response to microcystin-LR, a common form of cyanotoxin, which causes liver damage and disruption of lipid metabolism (Liu et al. 2014; Woolbright et al. 2017); and in the NAFLD zebrafish model, in accordance with mouse data in the literature (Cao et al. 2016; Yang et al. 2020). In our re-analysis, *ace2* expression in zebrafish refed liver steadily increased after fasting, aiding in the connection between *ace2* expression and diet. *Ace2* levels have also been shown to be elevated in high-fat-fed mice and rats (Gupte et al. 2008; Shoemaker et al. 2019; Zhang et al. 2014), but not in the initial response to lipid exposure in zebrafish digestive organs (Zeituni et al. 2016). This suggests that further experiments are needed to identify the time frame in which the diet can alter *ace2* levels in zebrafish. In addition to altered lipid metabolism, interferon pathway modulation (ISG15 antiviral mechanism network) has emerged as a discriminator of the low and high *ace2* expressing liver in zebrafish. The liver, an organ continually subjected to food antigens and pathogens from the intestines, can respond to such activators of immune response readily with its residential macrophages (Bleriot and Ginhoux 2019), which may result in highly variable interferon activity in the liver (reviewed in Robinson et al. 2016). Future studies focusing on embryonic and tissue-specific *ace2* knockout and overexpression models can help understand the role of adaptive and innate immune system challenges in zebrafish liver expression variability. Moreover, a significant decrease in *ace2* levels in response to vitamin D treatment during early development can be studied further in different contexts, including COVID-19 (Benskin 2020; Bleizgys 2021; Musavi et al. 2020; Ali et al. 2018; Andersen et al. 2015; Shen et al. 2017).

From a disease perspective, the observed decrease in *ace2* expression in the zebrafish SBS model may indicate a link between decreased levels of *ace2* and inflammation, as widely observed in human SBS patients (Schall et al. 2017). Our re-analysis showed that zebrafish *uhrf1* and *cdipt* mutants, with elevated intestinal inflammation, both exhibited a significant decrease in *ace2* expression (Marjoram et al. 2015; Thakur et al. 2014). In human inflammatory bowel disease (IBD), *ACE2* levels exhibit a similar decrease in inflamed ileum but increase in inflamed colon and rectum (Suarez-Farinas et al. 2020; Verstockt et al. 2021). In addition, zebrafish embryos deficient in the key innate immunity regulatory factor *myd88* exhibit altered lipid metabolism while expressing *ace2* highly, regardless of the type of microbiome (Koch et al. 2018). Interestingly, in mice, *MyD88* is essential for protection against SARS-CoV (Hirano and Murakami 2020; Sheahan et al. 2008). Moreover, our bioinformatics analyses showed that preexposure to the immune-suppressive and lipid modulatory agent β-glucans may lower *ace2* levels (AbuMweis et al. 2010), which supports an association between ace2 levels and modulation of inflammatory pathways, which remains to be tested.

We observed a sexually dimorphic expression pattern of *ace2* in zebrafish, which can provide a model for studying gender-specific *ace2* expression in response to different drugs with regard to hypertension and COVID-19 treatment (Cuffe et al. 2016; Goyal et al. 2015). Moreover, *esr2a* knockout zebrafish, exhibiting a significantly lower female-to-male offspring ratio (Lu et al. 2017; Wu et al. 2020), also showed lower *ace2* levels. Previously, a modulatory role of estrogen on *ACE2*

expression through its receptors, *ESR1* or *GPER1*, has been shown (Feng et al. 2020; Mompeon et al. 2016; Sun et al. 2021). Altogether, our analyses suggest a gender-specific role for *ace2* in zebrafish.

In conclusion, tissue- and context-dependent expression of *ace2* in zebrafish correlates well with human, non-human primate, and rodent data, as exemplified above. Moreover, via meta-analysis, we provide novel links between *ace2* expression modulation and diseases of the intestines and liver for the first time in the zebrafish literature. Our application of logFC-based extraction of co-expressed genes in zebrafish *ace2* translates into functional networks connected with each other via their common components. These networks were obtained based on heterogeneous datasets, hence reveal a relatively wide range of conditions zebrafish *ace2* expression could be modulated. A similar meta-analysis approach has been used in drug or compound networks, and herein applied to zebrafish *ace2*; hence, it is easily applicable to species-specific gene networks reflecting differential expression. Furthermore, we provide novel leads for testing zebrafish *ace2* levels against different drugs within a given developmental and physiological time frame, as well as different liver and intestinal pathologies.

Competing interests

The authors declare no competing or financial interests.

References

Abumweis, S.S., Jew, S., and Ames, N.P. 2010. β-glucan from barley and its lipid-lowering capacity: a meta-analysis of randomized, controlled trials. Eur. J. Clin. Nutr. **64**: 1472–1480. doi:10.1038/ejcn.2010.178. PMID:20924392.

Ali, R.M., Al-Shorbagy, M.Y., Helmy, M.W., and EL-Abhar, H.S. 2018. Role of Wnt4/beta-catenin, Ang II/TGFbeta, ACE2, NF-kappaB, and IL-18 in attenuating renal ischemia/reperfusion-induced injury in rats treated with Vit D and pioglitazone. Eur. J. Pharmacol. **831**: 68–76. doi:10.1016/j.ejphar.2018.04.032. PMID:29715453.

Alvarez-Rodriguez, M., Pereiro, P., Reyes-Lopez, F.E., Tort, L., Figueras, A., and Novoa, B. 2018. Analysis of the long-lived responses induced by immunostimulants and their effects on a viral infection in zebrafish (*Danio rerio*). Front. Immunol. **9**: 1575. doi:10.3389/fimmu.2018.01575. PMID:30038625.

Anders, S., Pyl, P.T., and Huber, W. 2015. HTSeq–a Python framework to work with high-throughput sequencing data. Bioinformatics, **31**: 166–169. doi:10.1093/bioinformatics/btu638. PMID:25260700.

Andersen, L.B., Przybyl, L., Haase, N., VON Versen-Hoynck, F., Qadri, F., Jorgensen, J.S., et al. 2015. Vitamin D depletion aggravates hypertension and target-organ damage. J. Am. Heart Assoc. **4**: e001417. doi:10.1161/JAHA.114.001417. PMID:25630909.

Aramillo Irizar, P., Schauble, S., Esser, D., Groth, M., Frahm, C., Priebe, S., et al. 2018. Transcriptomic alterations during ageing reflect the shift from cancer to degenerative diseases in the elderly. Nat. Commun. **9**: 327. doi:10.1038/s41467-017-02395-2. PMID:29382830.

Barrett, T., Wilhite, S.E., Ledoux, P., Evangelista, C., Kim, I.F., Tomashevsky, M., et al. 2013. NCBI GEO: archive for functional genomics data sets–update. Nucleic Acids Res. **41**: D991–D995. doi:10.1093/nar/gks1193. PMID:23193258.

Benskin, L.L. 2020. A basic review of the preliminary evidence that COVID-19 risk and severity is increased in vitamin D deficiency. Front. Publ. Health, **8**: 513. doi:10.3389/fpubh.2020.00513. PMID:33014983.

Bleizgys, A. 2021. Vitamin D and COVID-19: It is time to act. Int. J. Clin. Pract. **75**: e13748. doi:10.1111/ijcp.13748. PMID:33012103.

Bleriot, C., and Ginhoux, F. 2019. Understanding the heterogeneity of resident liver macrophages. Front. Immunol. **10**: 2694. doi:10.3389/fimmu.2019.02694. PMID:31803196.

Cao, X., Yang, F.Y., Xin, Z., Xie, R.R., and Yang, J.K. 2014. The ACE2/Ang-(1-7)/Mas axis can inhibit hepatic insulin resistance. Mol. Cell Endocrinol. **393**: 30–38. doi:10.1016/j.mce.2014.05.024. PMID:24911884.

Cao, X., Yang, F., Shi, T., Yuan, M., Xin, Z., Xie, R., et al. 2016. Angiotensin-converting enzyme 2/angiotensin-(1-7)/Mas axis activates Akt signaling to ameliorate hepatic steatosis. Sci. Rep. **6**: 21592. doi:10.1038/srep21592. PMID:26883384.

Cao, X., Lu, X.M., Tuo, X., Liu, J.Y., Zhang, Y.C., Song, L.N., et al. 2019. Angiotensin-converting enzyme 2 regulates endoplasmic reticulum stress and mitochondrial function to preserve skeletal muscle lipid metabolism. Lipids Health Dis. **18**: 207. doi:10.1186/s12944-019-1145-x. PMID:31775868.

Chen, L., Marishta, A., Ellison, C.E., and Verzi, M.P. 2020*a*. Identification of transcription factors regulating SARS-CoV-2 entry genes in the intestine. Cell. Mol. Gastroenterol. Hepatol. **11**: 181–184. doi:10.1016/j.jcmgh.2020.08.005. PMID:3281059.

Chen, L., Wang, L., Cheng, Q., Tu, Y.X., Yang, Z., Li, R.Z., et al. 2020*b*. Anti-masculinization induced by aromatase inhibitors in adult female zebrafish. BMC Genomics, **21**: 22. doi:10.1186/s12864-019-6437-z. PMID:31910818.

Cheng, Z., and Liu, Z. 2019. Renin-angiotensin system gene polymorphisms and colorectal cancer risk: a meta-analysis. J. Renin. Angiotensin. Aldosterone Syst. **20**: 1470320319881932. doi:10.1177/1470320319881932. PMID:31642377.

Cheng, J., and Yang, L. 2013. Comparing gene expression similarity metrics for connectivity map. *In* 2013 IEEE International Conference on Bioinformatics and Biomedicine, Dec. 18–21, 2013, Shanghai, China. pp. 165–170.

Cheng, P.Y., Lin, C.C., Wu, C.S., Lu, Y.F., Lin, C.Y., Chung, C.C., et al. 2008. Zebrafish cdx1b regulates expression of downstream factors of Nodal signaling during early endoderm formation. Development, **135**: 941–952. doi:10.1242/dev.010595. PMID:18234726.

Cheung, M.W., and Vijayakumar, R. 2016. A guide to conducting a meta-analysis. Neuropsychol. Rev. **26**: 121–128. doi:10.1007/s11065-016-9319-z. PMID:27209412.

Chou, C.F., Loh, C.B., Foo, Y.K., Shen, S., Fielding, B.C., Tan, T.H., et al. 2006. ACE2 orthologues in non-mammalian vertebrates (*Danio*, *Gallus*, *Fugu*, *Tetraodon* and *Xenopus*). Gene, **377**: 46–55. doi:10.1016/j.gene.2006.03.010. PMID:16781089.

Coccheri, S. 2020. COVID-19: The crucial role of blood coagulation and fibrinolysis. Intern. Emerg. Med. **15**: 1369–1373. doi:10.1007/s11739-020-02443-8. PMID:32748128.

Cuffe, J.S., Burgess, D.J., O'Sullivan, L., Singh, R.R., and Moritz, K.M. 2016. Maternal corticosterone exposure in the mouse programs sex-specific renal adaptations in the renin-angiotensin-aldosterone system in 6-month offspring. Physiol. Rep. **4**: e12754. doi:10.14814/phy2.12754. PMID:27122048.

Dobin, A., Davis, C.A., Schlesinger, F., Drenkow, J., Zaleski, C., Jha, S., et al. 2013. STAR: ultrafast universal RNA-seq aligner. Bioinformatics, **29**: 15–21. doi:10.1093/bioinformatics/bts635. PMID:23104886.

Domazet-Loso, T., and Tautz, D. 2010. A phylogenetically based transcriptome age index mirrors ontogenetic divergence patterns. Nature, **468**: 815–818. doi:10.1038/nature09632. PMID:21150997.

Evangelou, E., and Ioannidis, J.P. 2013. Meta-analysis methods for genome-wide association studies and beyond. Nat. Rev. Genet. **14**: 379–389. doi:10.1038/nrg3472. PMID:23657481.

Feng, Q., Li, L., and Wang, X. 2020. Identifying pathways and networks associated with the SARS-CoV-2 cell receptor ACE2 based on gene expression profiles in normal and SARS-CoV-2-infected human tissues. Front. Mol. Biosci. **7**: 568954. doi:10.3389/fmolb.2020.568954. PMID:33195414.

Flores, M.V., Hall, C.J., Davidson, A.J., Singh, P.P., Mahagaonkar, A.A., Zon, L.I., et al. 2008. Intestinal differentiation in zebrafish requires Cdx1b, a functional equivalent of mammalian Cdx2. Gastroenterology, **135**: 1665–1675. doi:10.1053/j.gastro.2008.07.024. PMID:18804112.

Forn-Cuni, G., Varela, M., Pereiro, P., Novoa, B., and Figueras, A. 2017. Conserved gene regulation during acute inflammation between zebrafish and mammals. Sci. Rep. **7**: 41905. doi:10.1038/srep41905. PMID:28157230.

Froehlicher, M., Liedtke, A., Groh, K., Lopez-Schier, H., Neuhauss, S.C., Segner, H., and Eggen, R.I. 2009. Estrogen receptor subtype beta2 is involved in neuromast development in zebrafish (*Danio rerio*) larvae. Dev. Biol. **330**: 32–43. doi:10.1016/j.ydbio.2009.03.005. PMID:19289112.

Gallagher, P.E., Ferrario, C.M., and Tallant, E.A. 2008. MAP kinase/phosphatase pathway mediates the regulation of ACE2 by angiotensin peptides. Am. J. Physiol. Cell. Physiol. **295**: C1169–74. doi:10.1152/ajpcell.00145.2008. PMID:18768926.

Ganz, J., Melancon, E., Wilson, C., Amores, A., Batzel, P., Strader, M., et al. 2019. Epigenetic factors Dnmt1 and Uhrf1 coordinate intestinal development. Dev. Biol. **455**: 473–484. doi:10.1016/j.ydbio.2019.08.002. PMID:31394080.

Gautier, L., Cope, L., Bolstad, B.M., and Irizarry, R.A. 2004. affy–analysis of Affymetrix GeneChip data at the probe level. Bioinformatics, **20**: 307–315. doi:10.1093/bioinformatics/btg405. PMID:14960456.

Gava, E., Samad-Zadeh, A., Zimpelmann, J., Bahramifarid, N., Kitten, G.T., Santos, R.A., et al. 2009. Angiotensin-(1-7) activates a tyrosine phosphatase and inhibits glucose-induced signalling in proximal tubular cells. Nephrol. Dial Transplant, **24**: 1766–1773. doi:10.1093/ndt/gfn736. PMID:19144997.

Gomes, M.C., and Mostowy, S. 2020. The case for modeling human infection in Zebrafish. Trends Microbiol. **28**: 10–18. doi:10.1016/j.tim.2019.08.005. PMID:31604611.

Goyal, R., VAN-Wickle, J., Goyal, D., and Longo, L.D. 2015. Antenatal maternal low protein diet: ACE-2 in the mouse lung and sexually dimorphic programming of hypertension. BMC Physiol. **15**: 2. doi:10.1186/s12899-015-0016-6. PMID:25971747.

Gupte, M., Boustany-Kari, C.M., Bharadwaj, K., Police, S., Thatcher, S., Gong, M.C., et al. 2008. ACE2 is expressed in mouse adipocytes and regulated by a high-fat diet. Am. J. Physiol. Regul. Integr. Comp. Physiol. **295**: R781–R788. doi:10.1152/ajpregu.00183.2008. PMID:18650320.

Gur-Dedeoglu, B., Konu, O., Kir, S., Ozturk, A.R., Bozkurt, B., Ergul, G., and Yulug, I.G. 2008. A resampling-based meta-analysis for detection of differential gene expression in breast cancer. BMC Cancer, **8**: 396. doi:10.1186/1471-2407-8-396. PMID:19116033.

Gwathmey, T.M., Pendergrass, K.D., Reid, S.D., Rose, J.C., Diz, D.I., and Chappell, M.C. 2010. Angiotensin-(1-7)-angiotensin-converting enzyme 2 attenuates reactive oxygen species formation to angiotensin II within the cell nucleus. Hypertension, **55**: 166–171. doi:10.1161/HYPERTENSIONAHA.109.141622. PMID:19948986.

Hamming, I., Cooper, M.E., Haagmans, B.L., Hooper, N.M., Korstanje, R., Osterhaus, A.D., et al. 2007. The emerging role of ACE2 in physiology and disease. J. Pathol. **212**: 1–11. doi:10.1002/path.2162. PMID:17464936.

Heiden, T.C., Struble, C.A., Rise, M.L., Hessner, M.J., Hutz, R.J., and Carvan, M.J., 3RD. 2008. Molecular targets of 2,3,7,8-tetrachlorodibenzo-p-dioxin (TCDD) within the zebrafish ovary: insights into TCDD-induced endocrine disruption and reproductive toxicity. Reprod. Toxicol. **25**: 47–57. doi:10.1016/j.reprotox.2007.07.013. PMID:17884332.

Hirano, T., and Murakami, M. 2020. COVID-19: a new virus, but a familiar receptor and cytokine release syndrome. Immunity, **52**: 731–733. doi:10.1016/j.immuni.2020.04.003. PMID:32325025.

Holden, L.A., and Brown, K.H. 2018. Baseline mRNA expression differs widely between common laboratory strains of zebrafish. Sci. Rep. **8**: 4780. doi:10.1038/s41598-018-23129-4. PMID:29555936.

Hu, B., Chen, H., Liu, X., Zhang, C., Cole, G.J., Lee, J.A., and Chen, X. 2013. Transgenic overexpression of cdx1b induces metaplastic changes of gene expression in zebrafish esophageal squamous epithelium. Zebrafish, **10**: 218–227. doi:10.1089/zeb.2012.0784. PMID:23672288.

Jacob, V., Chernyavskaya, Y., Chen, X., Tan, P.S., Kent, B., Hoshida, Y., and Sadler, K.C. 2015. DNA hypomethylation induces a DNA replication-associated cell cycle arrest to block hepatic outgrowth in uhrf1 mutant zebrafish embryos. Development, **142**: 510–521. doi:10.1242/dev.115980. PMID:25564650.

Jia, H.P., Look, D.C., Shi, L., Hickey, M., Pewe, L., Netland, J., Jr., et al. 2005. ACE2 receptor expression and severe acute respiratory syndrome coronavirus infection depend on differentiation of human airway epithelia. J. Virol. **79**: 14614–14621. doi:10.1128/JVI.79.23.14614-14621.2005. PMID:16282461.

Jia, J., Qin, J., Yuan, X., Liao, Z., Huang, J., Wang, B., et al. 2019. Microarray and metabolome analysis of hepatic response to fasting and subsequent refeeding in zebrafish (*Danio rerio*). BMC Genomics, **20**: 919. doi:10.1186/s12864-019-6309-6. PMID:31791229.

Johnson, E., Vu, L., and Matarese, L.E. 2018. Bacteria, bones, and stones: managing complications of short bowel syndrome. Nutr. Clin. Pract. **33**: 454–466. doi:10.1002/ncp.10113. PMID:29926935.

Kim, S.M., Kim, Y.G., Jeong, K.H., Lee, S.H., Lee, T.W., Ihm, C.G., and Moon, J.Y. 2012. Angiotensin II-induced mitochondrial Nox4 is a major endogenous source of oxidative stress in kidney tubular cells. PLoS ONE, **7**: e39739. doi:10.1371/journal.pone.0039739. PMID:22808054.

Kimmel, C.B., Ballard, W.W., Kimmel, S.R., Ullmann, B., and Schilling, T.F. 1995. Stages of embryonic development of the zebrafish. Dev. Dyn. **203**: 253–310. doi:10.1002/aja.1002030302. PMID:8589427.

Koch, B.E.V., Yang, S., Lamers, G., Stougaard, J., and Spaink, H.P. 2018. Intestinal microbiome adjusts the innate immune setpoint during colonization through negative regulation of MyD88. Nat. Commun. **9**: 4099. doi:10.1038/s41467-018-06658-4. PMID:30291253.

Kolde, R., Laur, S., Adler, P., and Vilo, J. 2012. Robust rank aggregation for gene list integration and meta-analysis. Bioinformatics, **28**: 573–580. doi:10.1093/bioinformatics/btr709. PMID:22247279.

Kramer, S., Busch, W., and Schuttler, A. 2020. A self-organizing map of the fathead minnow liver transcriptome to identify consistent toxicogenomic patterns across chemical fingerprints. Environ. Toxicol. Chem. **39**: 526–537. doi:10.1002/etc.4646. PMID:31820487.

Kryuchkova-Mostacci, N., and Robinson-Rechavi, M. 2017. A benchmark of gene expression tissue-specificity metrics. Brief. Bioinform. **18**: 205–214. doi:10.1093/bib/bbw008. PMID:26891983.

Lee, I.T., Nakayama, T., Wu, C.T., Goltsev, Y., Jiang, S., Gall, P.A., et al. 2020*a*. ACE2 localizes to the respiratory cilia and is not

increased by ACE inhibitors or ARBs. Nat. Commun. **11**: 5453. doi:10.1038/s41467-020-19145-6. PMID:33116139.

Lee, I.T., Nakayama, T., Wu, C.T., Goltsev, Y., Jiang, S., Gall, P.A., et al. 2020*b*. Robust ACE2 protein expression localizes to the motile cilia of the respiratory tract epithelia and is not increased by ACE inhibitors or angiotensin receptor blockers. medRxiv. [In press.] doi:10.1101/2020.05.08.20092866. PMID: 32511516.

Liu, W., Qiao, Q., Chen, Y., Wu, K., and Zhang, X. 2014. Microcystin-LR exposure to adult zebrafish (*Danio rerio*) leads to growth inhibition and immune dysfunction in F1 offspring, a parental transmission effect of toxicity. Aquat. Toxicol. **155**: 360–367. doi:10.1016/j.aquatox.2014.07.011. PMID: 25105566.

Logan, S.L., Thomas, J., Yan, J., Baker, R.P., Shields, D.S., Xavier, J.B., et al. 2018. The Vibrio cholerae type VI secretion system can modulate host intestinal mechanics to displace gut bacterial symbionts. Proc. Natl. Acad. Sci. U.S.A. **115**: E3779–E3787. doi:10.1073/pnas.1720133115. PMID:29610339.

Love, M.I., Huber, W., and Anders, S. 2014. Moderated estimation of fold change and dispersion for RNA-seq data with DESeq2. Genome Biol. **15**: 550. doi:10.1186/s13059-014-0550-8. PMID:25516281.

Lu, H., Cui, Y., Jiang, L., and Ge, W. 2017. Functional analysis of nuclear estrogen receptors in zebrafish reproduction by genome editing approach. Endocrinology, **158**: 2292–2308. doi:10.1210/en.2017-00215. PMID:28398516.

MacInnes, A.W., Amsterdam, A., Whittaker, C.A., Hopkins, N., and Lees, J.A. 2008. Loss of p53 synthesis in zebrafish tumors with ribosomal protein gene mutations. Proc. Natl. Acad. Sci. U.S.A. **105**: 10408–10413. doi:10.1073/pnas.0805036105. PMID: 18641120.

Marjoram, L., Alvers, A., Deerhake, M.E., Bagwell, J., Mankiewicz, J., Cocchiaro, J.L., et al. 2015. Epigenetic control of intestinal barrier function and inflammation in zebrafish. Proc. Natl. Acad. Sci. U.S.A. **112**: 2770–2775. doi:10.1073/pnas.1424089112. PMID:25730872.

McCarthy, D.J., Chen, Y., and Smyth, G.K. 2012. Differential expression analysis of multifactor RNA-Seq experiments with respect to biological variation. Nucleic Acids Res. **40**: 4288–4297. doi:10.1093/nar/gks042. PMID:22287627.

Mickiewicz, K.M., Kawai, Y., Drage, L., Gomes, M.C., Davison, F., Pickard, R., et al. 2019. Possible role of L-form switching in recurrent urinary tract infection. Nat. Commun. **10**: 4379. doi:10.1038/s41467-019-12359-3. PMID:31558767.

Mompeon, A., Lazaro-Franco, M., Bueno-Beti, C., Perez-Cremades, D., Vidal-Gomez, X., Monsalve, E., et al. 2016. Estradiol, acting through ERalpha, induces endothelial non-classic renin-angiotensin system increasing angiotensin 1-7 production. Mol. Cell. Endocrinol. **422**: 1–8. doi:10.1016/j.mce.2015.11.004. PMID:26562171.

Musavi, H., Abazari, O., Barartabar, Z., Kalaki-Jouybari, F., Hemmati-Dinarvand, M., Esmaeili, P., and Mahjoub, S. 2020. The benefits of Vitamin D in the COVID-19 pandemic: biochemical and immunological mechanisms. Arch. Physiol. Biochem. pp. 1–9. [In press.] doi:10.1080/13813455.2020.1826530. PMID:33030073.

Mutanen, A., Barrett, M., Feng, Y., Lohi, J., Rabah, R., Teitelbaum, D.H., and Pakarinen, M.P. 2019. Short bowel mucosal morphology, proliferation and inflammation at first and repeat STEP procedures. J. Pediatr. Surg. **54**: 511–516. doi:10.1016/j.jpedsurg.2018.04.016. PMID:29753524.

Nehme, A., Zouein, F.A., Zayeri, Z.D., and Zibara, K. 2019. An Update on the tissue renin angiotensin system and its role in physiology and pathology. J. Cardiovasc. Dev. Dis. **6**: 14. doi:10.3390/jcdd6020014. PMID:30934934.

Okuda, Y., Ogura, E., Kondoh, H., and Kamachi, Y. 2010. B1 SOX coordinate cell specification with patterning and morphogenesis in the early zebrafish embryo. PLoS Genet, **6**: e1000936. doi:10.1371/journal.pgen.1000936. PMID:20463883.

Papatheodorou, I., Moreno, P., Manning, J., Fuentes, A.M., George, N., Fexova, S., et al. 2020. Expression Atlas update: from tissues to single cells. Nucleic Acids Res. **48**: D77–D83. doi:10.1093/nar/gkz947. PMID:31665515.

Pinter, M., and Jain, R.K. 2017. Targeting the renin-angiotensin system to improve cancer treatment: Implications for immunotherapy. Sci. Transl. Med. **9**: eaan5616. doi:10.1126/scitranslmed.aan5616. PMID:28978752.

Postlethwait, J.H., Massaquoi, M.S., Farnsworth, D.R., Yan, Y.L., Guillemin, K., and Miller, A.C. 2021. The SARS-CoV-2 receptor and other key components of the Renin-Angiotensin-Aldosterone System related to COVID-19 are expressed in enterocytes in larval zebrafish. Biol. Open, **10**: bio058172. doi:10.1242/bio.058172. PMID:33757938.

Rasha, F., Ramalingam, L., Gollahon, L., Rahman, R.L., Rahman, S.M., Menikdiwela, K., and Moustaid-Moussa, N. 2019. Mechanisms linking the renin-angiotensin system, obesity, and breast cancer. Endocr. Relat. Cancer, **26**: R653–R672. doi:10.1530/ERC-19-0314. PMID:31525726.

Ritchie, M.E., Phipson, B., Wu, D., Hu, Y., Law, C.W., Shi, W., and Smyth, G.K. 2015. limma powers differential expression analyses for RNA-sequencing and microarray studies. Nucleic Acids Res. **43**: e47. doi:10.1093/nar/gkv007. PMID: 25605792.

Robinson, M.W., Harmon, C., and O'Farrelly, C. 2016. Liver immunology and its role in inflammation and homeostasis. Cell. Mol. Immunol. **13**: 267–276. doi:10.1038/cmi.2016.3. PMID:27063467.

Robison, B.D., Drew, R.E., Murdoch, G.K., Powell, M., Rodnick, K.J., Settles, M., et al. 2008. Sexual dimorphism in hepatic gene expression and the response to dietary carbohydrate manipulation in the zebrafish (Danio rerio). Comp. Biochem. Physiol. Part D Genomics Proteomics, **3**: 141–154. doi:10.1016/j.cbd.2008.01.001. PMID:20483215.

Rogers, E.D., Henry, T.B., Twiner, M.J., Gouffon, J.S., Mcpherson, J.T., Boyer, G.L., et al. 2011. Global gene expression profiling in larval zebrafish exposed to microcystin-LR and microcystis reveals endocrine disrupting effects of cyanobacteria. Environ. Sci. Technol. **45**: 1962–1969. doi:10.1021/es103538b. PMID:21280650.

San, B., Aben, M., Elurbe, D.M., Voeltzke, K., DEN Broeder, M.J., Rougeot, J., et al. 2018. Genetic and epigenetic regulation of zebrafish intestinal development. Epigenomes, **2**: 19. doi:10.3390/epigenomes2040019.

Schall, K.A., Thornton, M.E., Isani, M., Holoyda, K.A., Hou, X., Lien, C.L., et al. 2017. Short bowel syndrome results in increased gene expression associated with proliferation, inflammation, bile acid synthesis and immune system activation: RNA sequencing a zebrafish SBS model. BMC Genomics, **18**: 23. doi:10.1186/s12864-016-3433-4. PMID: 28118819.

Shannon, P., Markiel, A., Ozier, O., Baliga, N.S., Wang, J.T., Ramage, D., et al. 2003. Cytoscape: a software environment for integrated models of biomolecular interaction networks. Genome Res. **13**: 2498–2504. doi:10.1101/gr.1239303. PMID:14597658.

Sheahan, T., Morrison, T.E., Funkhouser, W., Uematsu, S., Akira, S., Baric, R.S., and Heise, M.T. 2008. MyD88 is required for protection from lethal infection with a mouse-adapted SARS-CoV. PLoS Pathog. **4**: e1000240. doi:10.1371/journal.ppat.1000240. PMID:19079579.

Shehwana, H., and Konu, O. 2019. Comparative transcriptomics between zebrafish and mammals: a roadmap for discovery of conserved and unique signaling pathways in physiology and disease. Front. Cell Dev. Biol. **7**: 5. doi:10.3389/fcell.2019.00005. PMID:30775367.

Shen, L., Ma, C., Shuai, B., and Yang, Y. 2017. Effects of 1,25-dihydroxyvitamin D3 on the local bone renin-angiotensin system in a murine model of glucocorticoid-induced osteoporosis. Exp. Ther. Med. **13**: 3297–3304. doi:10.3892/etm.2017.4404. PMID:28587403.

Shi, T.T., Yang, F.Y., Liu, C., Cao, X., Lu, J., Zhang, X.L., et al. 2018. Angiotensin-converting enzyme 2 regulates mitochondrial function in pancreatic beta-cells. Biochem. Biophys. Res. Commun. **495**: 860–866. doi:10.1016/j.bbrc.2017.11.055. PMID:29128354.

Shoemaker, R., Tannock, L.R., Su, W., Gong, M., Gurley, S.B., Thatcher, S.E., et al. 2019. Adipocyte deficiency of ACE2 increases systolic blood pressures of obese female C57BL/6 mice. Biol. Sex Differ. **10**: 45. doi:10.1186/s13293-019-0260-8. PMID:31484552.

Silberg, D.G., Swain, G.P., Suh, E.R., and Traber, P.G. 2000. Cdx1 and cdx2 expression during intestinal development. Gastroenterology, **119**: 961–971. doi:10.1053/gast.2000.18142. PMID:11040183.

Small, C.M., Carney, G.E., Mo, Q., Vannucci, M., and Jones, A.G. 2009. A microarray analysis of sex- and gonad-biased gene expression in the zebrafish: evidence for masculinization of the transcriptome. BMC Genomics, **10**: 579. doi:10.1186/1471-2164-10-579. PMID:19958554.

Song, R., Preston, G., and Yosypiv, I.V. 2012. Ontogeny of angiotensin-converting enzyme 2. Pediatr. Res. **71**: 13–19. doi:10.1038/pr.2011.7. PMID:22289845.

Song, L.N., Liu, J.Y., Shi, T.T., Zhang, Y.C., Xin, Z., Cao, X., and Yang, J.K. 2020. Angiotensin-(1-7), the product of ACE2 ameliorates NAFLD by acting through its receptor Mas to regulate hepatic mitochondrial function and glycolipid metabolism. FASEB J. **34**: 16291–16306. doi:10.1096/fj.202001639R. PMID:33078906.

Soni, K., Choudhary, A., Patowary, A., Singh, A.R., Bhatia, S., Sivasubbu, S., et al. 2013. miR-34 is maternally inherited in Drosophila melanogaster and Danio rerio. Nucleic Acids Res. **41**: 4470–4480. doi:10.1093/nar/gkt139. PMID:23470996.

Stuckenholz, C., Lu, L., Thakur, P., Kaminski, N., and Bahary, N. 2009. FACS-assisted microarray profiling implicates novel genes and pathways in zebrafish gastrointestinal tract development. Gastroenterology, **137**: 1321–1332. doi:10.1053/j.gastro.2009.06.050. PMID:19563808.

Suarez-Farinas, M., Tokuyama, M., Wei, G., Huang, R., Livanos, A., Jha, D., et al. 2020. Intestinal inflammation modulates the expression of ACE2 and TMPRSS2 and potentially overlaps with the pathogenesis of SARS-CoV-2 related disease. Gastroenterology, **160**: 287–301.e20. doi:10.1053/j.gastro.2020.09.029. PMID:32980345.

Sun, X., Wang, H., Hodge, H., Wright, K.N., Ahmad, S., Ferrario, C.M., and Groban, L. 2021. Amplifying effect of chronic lisinopril therapy on diastolic function and the angiotensin-(1-7) Axis by the G1 agonist in ovariectomized spontaneously hypertensive rats. Transl. Res. **235**: 62–76. doi:10.1016/j.trsl.2021.04.004. PMID:33915312.

Szklarczyk, D., Franceschini, A., Wyder, S., Forslund, K., Heller, D., Huerta-Cepas, J., et al. 2015. STRING v10: protein-protein interaction networks, integrated over the tree of life. Nucleic Acids Res. **43**: D447–D452. doi:10.1093/nar/gku1003. PMID:25352553.

Szklarczyk, D., Gable, A.L., Lyon, D., Junge, A., Wyder, S., Huerta-Cepas, J., et al. 2019. STRING v11: protein-protein association networks with increased coverage, supporting functional discovery in genome-wide experimental datasets. Nucleic Acids Res. **47**: D607–D613. doi:10.1093/nar/gky1131. PMID:30476243.

Ter Veer, E., Van Oijen, M.G.H., and Van Laarhoven, H.W.M. 2019. The use of (network) meta-analysis in clinical oncology. Front. Oncol. **9**: 822. doi:10.3389/fonc.2019.00822. PMID:31508373.

Thakur, P.C., Davison, J.M., Stuckenholz, C., Lu, L., and Bahary, N. 2014. Dysregulated phosphatidylinositol signaling promotes endoplasmic-reticulum-stress-mediated intestinal mucosal injury and inflammation in zebrafish. Dis. Model. Mech. **7**: 93–106. doi:10.1242/dmm.012864. PMID:24135483.

Tseng, G.C., Ghosh, D., and Feingold, E. 2012. Comprehensive literature review and statistical considerations for microarray meta-analysis. Nucleic Acids Res. **40**: 3785–3799. doi:10.1093/nar/gkr1265. PMID:22262733.

Vargas, M., Servillo, G., and Einav, S. 2020. Lopinavir/ritonavir for the treatment of SARS, MERS and COVID-19: a systematic review. Eur. Rev. Med. Pharmacol. Sci. **24**: 8592–8605. doi:10.26355/eurrev_202008_22659. PMID:32894567.

Verstockt, B., Verstockt, S., Abdu Rahiman, S., Ke, B.J., Arnauts, K., Cleynen, I., et al. 2021. Intestinal receptor of SARS-CoV-2 in inflamed IBD tissue seems downregulated by HNF4A in ileum and upregulated by interferon regulating factors in colon. J. Crohns Colitis, **15**: 485–498. doi:10.1093/ecco-jcc/jjaa185. PMID:32915959.

Wang, Y., Wang, Y., Luo, W., Huang, L., Xiao, J., Li, F., et al. 2020. A comprehensive investigation of the mRNA and protein level of ACE2, the putative receptor of SARS-CoV-2, in human tissues and blood cells. Int. J. Med. Sci. **17**: 1522–1531. doi:10.7150/ijms.46695. PMID:32669955.

White, R.J., Collins, J.E., Sealy, I.M., Wali, N., Dooley, C.M., Digby, Z., et al. 2017. A high-resolution mRNA expression time course of embryonic development in zebrafish. eLife, **6**: e30860. doi:10.7554/eLife.30860. PMID:29144233.

Willis, A.R., Moore, C., Mazon-Moya, M., Krokowski, S., Lambert, C., Till, R., et al. 2016. Injections of predatory bacteria work alongside host immune cells to treat *Shigella* infection in zebrafish larvae. Curr. Biol. **26**: 3343–3351. doi:10.1016/j.cub.2016.09.067. PMID:27889262.

Woolbright, B.L., Williams, C.D., Ni, H., Kumer, S.C., Schmitt, T., Kane, B., and Jaeschke, H. 2017. Microcystin-LR induced liver injury in mice and in primary human hepatocytes is caused by oncotic necrosis. Toxicon, **125**: 99–109. doi:10.1016/j.toxicon.2016.11.254. PMID:27889601.

Wu, K., Song, W., Zhang, Z., and Ge, W. 2020. Disruption of dmrt1 rescues the all-male phenotype of the cyp19a1a mutant in zebrafish - a novel insight into the roles of aromatase/estrogens in gonadal differentiation and early folliculogenesis. Development, **147**: dev182758. doi:10.1242/dev.182758. PMID:32001440.

Yang, M., Ma, X., Xuan, X., Deng, H., Chen, Q., and Yuan, L. 2020. Liraglutide attenuates non-alcoholic fatty liver disease in mice by regulating the local renin-angiotensin system. Front. Pharmacol. **11**: 432. doi:10.3389/fphar.2020.00432. PMID:32322207.

Yao, T.T., Qian, J.D., Zhu, W.Y., Wang, Y., and Wang, G.Q. 2020. A systematic review of lopinavir therapy for SARS coronavirus and MERS coronavirus - a possible reference for coronavirus disease-19 treatment option. J. Med. Virol. **92**: 556–563. doi:10.1002/jmv.25729. PMID:32104907.

Yildiz, G., Arslan-Ergul, A., Bagislar, S., Konu, O., Yuzugullu, H., Gursoy-Yuzugullu, O., et al. 2013. Genome-wide transcriptional reorganization associated with senescence-to-immortality switch during human hepatocellular carcinogenesis. PLoS ONE, **8**: e64016. doi:10.1371/journal.pone.0064016. PMID:23691139.

Yoon, S., Nguyen, H.C.T., Jo, W., Kim, J., Chi, S.M., Park, J., et al. 2019. Biclustering analysis of transcriptome big data identifies condition-specific microRNA targets. Nucleic Acids Res. **47**: e53. doi:10.1093/nar/gkz139. PMID:30820547.

Yu, G., Wang, L.G., Han, Y., and He, Q.Y. 2012. clusterProfiler: an R package for comparing biological themes among gene

clusters. OMICS, **16**: 284–287. doi:10.1089/omi.2011.0118. PMID: 22455463.

Yuan, J., Fan, D., Xue, Z., Qu, J., and Su, J. 2020. Co-expression of mitochondrial genes and ACE2 in cornea involved in COVID-19. Invest. Ophthalmol. Vis. Sci. **61**: 13. doi:10.1167/iovs.61.12.13. PMID:33049061.

Zeituni, E.M., Wilson, M.H., Zheng, X., Iglesias, P.A., Sepanski, M.A., Siddiqi, M.A., et al. 2016. Endoplasmic Reticulum Lipid Flux Influences Enterocyte Nuclear Morphology and Lipid-dependent Transcriptional Responses. J. Biol. Chem. **291**: 23804–23816. doi:10.1074/jbc.M116.749358. PMID:27655916.

Zhang, W., Xu, Y.Z., Liu, B., Wu, R., Yang, Y.Y., Xiao, X.Q., and Zhang, X. 2014. Pioglitazone upregulates angiotensin converting enzyme 2 expression in insulin-sensitive tissues in rats with high-fat diet-induced nonalcoholic steatohepatitis. Sci. World J. **2014**: 603409. doi:10.1155/2014/603409. PMID:24558317.

Zhou, X., Wang, M., Katsyv, I., Irie, H., and Zhang, B. 2018. EMUDRA: ensemble of multiple drug repositioning approaches to improve prediction accuracy. Bioinformatics, **34**: 3151–3159. doi:10.1093/bioinformatics/bty325. PMID:29688306.

Ziegler, C.G.K., Allon, S.J., Nyquist, S.K., Mbano, I.M., Miao, V.N., Tzouanas, C.N., et al. 2020. SARS-CoV-2 receptor ACE2 is an interferon-stimulated gene in human airway epithelial cells and is detected in specific cell subsets across tissues. Cell, **181**: 1016–1035. e19. doi:10.1016/j.cell.2020.04.035. PMID: 32413319.